Communication advantage of quantum compositions of channels from non-Markovianity

Jian Wei Cheong ⬤, Andri Pradana ⬤, and Lock Yue Chew ⬤[*]

Division of Physics and Applied Physics, School of Physical and Mathematical Sciences, Nanyang Technological University,
21 Nanyang Link, Singapore 637371

The combined use of quantum channels can grant communication advantages in the form of enhancements to communication capacities. One such channel composition is the quantum switch, which implements a system with indefinite causal order by coherent control of the orderings of two or more quantum channels, resulting in enhanced communication capacities. Here, using the monogamy relation, we studied the flow of entanglement monotone in these quantum compositions of channels in the environmental representation. We implemented the two-party quantum switch in this framework, and demonstrated that non-Markovianity is the source of revival of the entanglement monotone in this setup. The possibility and amount of revival was shown to depend on the entangling capability of the channels, and the perfect activation of coherent information with entanglement-breaking channels was also replicated with the perfect revival of entanglement monotone. Additionally, we showed that a more general non-Markovian circuit can still grant enhancements to coherent information and Holevo quantity without the presence of indefinite causal order.

I. INTRODUCTION

Quantum communication theory saw many surprising phenomena not present in classical communication theory due to the presence of entanglement, such as superdense coding [1], where quantum communication is used to enhance classical communication, and quantum teleportation [2], where classical communication is used to assist quantum communication. A large part of foundational works on quantum communication theory are on quantifying the maximum possible communication rates or capacities of these phenomena both with and without initial entanglement [3–9]. Similar to the classical capacity, the quantum capacity of a channel can be quantified by the rate of qubit transmission instead of bits. However, unlike the classical case, the combined use of quantum channels can lead to an enhancement of quantum capacity when used on an initially entangled state. For example, parallel use of a pair of quantum channels on a pair of entangled qubits can result in a superadditivity of capacities, where the overall quantum and classical capacities are greater than the sum of the individual channel capacities [10,11]. Furthermore, in what is known as superactivation, such an enhancement is possible for the quantum capacity even if the individual channels each has zero quantum capacity [12].

Different from superadditivity and superactivation, where the placement of quantum channels is fixed, there have been growing interests in the phenomenon of indefinite causal orders, where the orderings of two or more quantum operations are placed in a superposition of different orders [13]. Such a setup can be implemented by what is known as the quantum switch, which puts different orders of quantum operations

in a coherent superposition controlled by a control system [14]. The phenomenon of indefinite causal orders has seen multiple advantages in terms of computation [15–17], metrology [18–20], and refrigeration or work extraction [21,22] tasks. Such advantages also include enhancement to communication complexities in communication games, as well as enhancements to classical and quantum capacities as compared to using the channels in series, violating the bottleneck inequality [23–26]. Like superactivation, this enhancement is even possible if the individual channels have zero capacities [27,28]. While these enhancements are usually shown for the two-party quantum switch, where only two operations are placed in a superposition of two alternating orders, there are also works demonstrating enhancements for more than two parties in more than two superpositions of orders [29,30].

The enhancement of capacities by the quantum switch is referred to as causal activation, and the origins of this communication advantage have been a topic of debate. Particularly, it was shown that a controlled superposition of two independent channels can replicate and surpass the quantum switch's enhancement, suggesting that the ability to coherently control superposition might be more significant than the superposition of orders [31]. Reference [32] also demonstrated this for a more general class of controlled superposition known as superposition of direct pure processes, for which it was suggested that the fundamental resource behind the quantum switch is the coherent control of a superposition of operations rather than its indefinite causality. However, it was argued that these counterexamples have the presence of resources that are not present in the quantum switch, such as generating side channels, or using vacuum-extended channels that utilize the coherence with the vacuum state as a resource [33,34]. Also in support of the resource of indefinite causality in the quantum switch, Ref. [28] showed that the perfect activation of

---

[*]lockyue@ntu.edu.sg

quantum capacities on a pair of channels with zero capacities was only possible with the quantum switch's superposition of causal orders, and not in a superposition of independent channels or trajectories. Furthermore, Ref. [25] demonstrated numerically for arbitrary choices of channels that while implementing a controlled superposition of two independent channels always enhances communication, implementing the quantum switch can either grant a greater enhancement, or it can worsen the communication capacities, raising more questions on the origins of the resource utilized in the quantum switch. Similarly, on the experimental side of things, despite that the quantum switch has been implemented experimentally as a tabletop photonics setup, and verified to enhance the classical and quantum capacities [35–38], there are still some doubts as to whether these experimental implementations are genuine superpositions of causal orders [39].

At the same time, there are actually known situations where a reduction in information loss, and thus an enhancement to communication, can be expected and explained in an open quantum system. These occur in a non-Markovian quantum process [40]. As a noisy quantum channel is an open system where the information-carrying system can be thought to be interacting with an environment and losing information to it, a non-Markovian interaction can grant the possibility of a backflow of information where information flowed to the environment returns to the information-carrying system, resulting in an increase in capacity of the channel [41].

A non-Markovian system can exhibit memory effects during repeated uses of a channel where a use can be correlated to a previous use. In other words, the noise induced by the channel at different points in time is correlated. Such correlation in time was also shown to reproduce and even surpass the communication advantages of the quantum switch in Ref. [42], where a particle is sent to a channel in a superposition of two different times. Additionally, there have been growing interests in the connections between non-Markovianity and indefinite causal order. For example, it was shown in Ref. [43] from an operational approach that a process with indefinite causal order can be simulated by a measurement on the environment and conditioning the outcomes, given that there is initial system-environment entanglement, which indicates the presence of non-Markovianity. It was also shown in Ref. [44] that in quantum random walks where the dynamics of the reduced coin state is non-Markovian [45], by placing the walk's evolution operators in an indefinite causal order, there is an increase in non-Markovianity as compared to a fixed causal order. Even more recently, it was shown that for channels that are non-Markovian but do not offer backflow of information, known as eternally non-Markovian channels [46], such that its non-Markovianity is "hidden," placing these channels in the quantum switch setup can activate this hidden non-Markovianity to allow backflow of information [47].

These works either suggest that non-Markovianity can replicate the advantages of the quantum switch or its indefinite causality in the case of Refs. [42,43], or that the quantum switch can activate or enhance the non-Markovianity already present in the system in the case of Refs. [46,47]. However, here we demonstrate that a composition of quantum channels that implements the two-party quantum switch itself has intrinsic non-Markovianity in its operation, suggesting that

this non-Markovianity can play a part in causal activation or in the communication advantages of the quantum switch. Specifically, we show that there is a revival of an entanglement monotone between the information-carrying system and a reference system, which is dependent on the entangling capabilities of the quantum channels. Furthermore, we generalized the circuit such that its non-Markovianity can be controlled, and showed that the difference between a superposition of causal orders and a superposition of trajectories, as explored in Ref. [28], is due to the presence of this non-Markovianity. In this non-Markovian framework, it seems to suggest that non-Markovianity is a resource that is utilized by the quantum switch, and we demonstrate that enhancements to communication capacities can be achieved with non-Markovianity alone, without the presence of indefinite causal order.

This paper is structured as follows. We first review the definitions of non-Markovianity and its environmental representation in Sec. II. We also review the definitions of the classical and quantum channel capacities, as well as their relation to the entanglement monotone for which a revival can indicate the presence of non-Markovianity. In Sec. III, we focus on the dynamics of this entanglement monotone, defining its flow and dependence on the entangling capability of the operations in an example single-pass system. In Sec. IV, we apply this framework to the two-party quantum switch to demonstrate the presence of non-Markovianity via the revival of the entanglement monotone, and show that the revival depends on the entangling capability of the operations. We also replicated the perfect activation of quantum capacities explored in Ref. [28] with the perfect revival of the entanglement monotone, and lastly we show that a more general circuit composition without indefinite causal order can also grant enhancements to communication capacities.

II. NON-MARKOVIANITY

A. Divisibility and information backflow

A quantum channel in general is described by a completely positive and trace-preserving (CPTP) map. Under the action of such a channel with the CPTP map Φ, a distinguishability measure $D(\rho, \sigma)$ of a pair of quantum states ρ and σ is contractive [48]:

$$D(\Phi(\rho), \Phi(\sigma)) \leqslant D(\rho, \sigma). \tag{1}$$

If the map $\Phi(\tau, 0)$ that acts from $t = 0$ to $t = \tau$ is a Markovian process, it is divisible for all times $0 \leqslant t \leqslant \tau$ [49,50], i.e.,

$$\Phi(\tau, 0) = \Phi(\tau, t)\Phi(t, 0), \quad \forall \, 0 \leqslant t \leqslant \tau \tag{2}$$

where both $\Phi(\tau, t)$ and $\Phi(t, 0)$ are CPTP maps. This is called the divisibility property. Therefore, the contraction of the distinguishability measure D will be monotonic for the entire time τ. On the other hand, for a non-Markovian process with respect to a CPTP map $\bar{\Phi}(\tau, 0)$, there are times t where it cannot be divisible into individual CPTP operations, and thus the divisibility condition in Eq. (2) does not hold [51]. In this case, we say that $\bar{\Phi}(\tau, 0)$ is CP indivisible or that it violates CP divisibility at those times t. In other words, we might have $\bar{\Phi}(\tau, 0) = \Gamma(\tau, t)\Phi(t, 0)$ where $\Gamma(\tau, t)$ is not a CPTP operation. As there is no CPTP description of $\bar{\Phi}(\tau, 0)$ at those times

t, Eq. (1) need not hold for those times. Such revival where the monotonic relation is violated with $D(\rho_\tau, \sigma_\tau) \geqslant D(\rho_t, \sigma_t)$ where $\tau \geqslant t$ is referred to as the backflow of information from the environment to the system, and is also known as the BLP definition, named after Breuer, Laine, and Piilo who first demonstrated this in Ref. [52].

Therefore, a common measure for the non-Markovianity of a process is the amount of violations of the monotonicity of measure $D(\rho, \sigma)$, where D is usually taken to be the trace distance [52–54]. However, divergence measures such as the relative entropy $S(\rho \parallel \sigma)$ will also fulfill Eq. (1) [55,56]. Therefore, the Holevo quantity $\chi(\rho) = \sum_a p_a S(\rho_a \parallel \rho)$ which lower bounds the classical capacity [6,7] is also monotonic:

$$\sum_a p_a S(\Phi(\rho_a) \parallel \Phi(\rho)) \leqslant \sum_a p_a S(\rho_a \parallel \rho), \qquad (3)$$

$$\chi(\Phi(\rho)) \leqslant \chi(\rho), \qquad (4)$$

where $\rho = \sum_a p_a \rho_a$. Similarly, the coherent information I_c which lower bounds the quantum capacity [8,9] was also shown to be a monotone [5]. These distinguishability or divergence measures that are monotonic under CPTP maps are information monotones, and their monotonic nature defines the irreversible loss of information under the application of a noisy quantum channel. Other choices of the information monotone include the quantum Fisher information [57,58] (refer to Ref. [40] for a review of the different types of measures).

It is important to note that CP indivisibility does not imply information backflow or revival [59] in general. Processes that are CP indivisible but do not have information backflow are referred to as an eternally non-Markovian process [46,47]. Nonetheless, for our purpose, we refer to the violation of the divisibility property in Eq. (2) as a process that is non-Markovian. Specifically, we take a nonoperational approach where the indivisibility is caused by the presence of memory in the environmental representation.

B. Environmental representation

The violation of the divisibility property, and thus the presence of non-Markovianity, can be made apparent in the environmental representation as the presence of memory or correlations in the environment. Any CPTP map Φ acting on a state $\rho^Q \in \mathcal{H}^Q$ can be represented by an operation on a larger Hilbert space $\mathcal{H}^Q \otimes \mathcal{H}^E$ with the extended space $\mathcal{H}^E$ traced out [49,55]. This operation can be an isometry A that maps $A : \mathcal{H}^Q \to \mathcal{H}^Q \otimes \mathcal{H}^E$, known as the Stinespring representation, or a unitary U that maps $U : \mathcal{H}^Q \otimes \mathcal{H}^E \to \mathcal{H}^Q \otimes \mathcal{H}^E$, known as the environmental representation as the system E plays the role of the environment that system Q interacts unitarily with

$$\Phi(\rho^Q) = \mathrm{Tr}_E[U(\rho^Q \otimes \rho^E)U^\dagger], \qquad (5)$$

where the unitary $U \in \mathcal{H}^Q \otimes \mathcal{H}^E$. Therefore, for a Markovian process where the CPTP map is divisible between two time steps according to Eq. (2) with $\Phi = \Phi_2 \circ \Phi_1$ where Φ_1 and

Φ_2 are valid CPTP maps, we have

$$\Phi_1(\rho_0^Q) = \rho_1^Q = \mathrm{Tr}_E[U_1(\rho_0^Q \otimes \rho^E)U_1^\dagger], \qquad (6)$$

$$\Phi_2(\rho_1^Q) = \rho_2^Q = \mathrm{Tr}_N[U_2(\rho_1^Q \otimes \rho^N)U_2^\dagger] \qquad (7)$$

and the monotonicity of information monotones such as the coherent information holds:

$$I_c(\rho_2^Q) \leqslant I_c(\rho_1^Q) \leqslant I_c(\rho_0^Q), \qquad (8)$$

where the subscripts denote the time steps.

A necessary condition for the environmental representation of a CPTP map to hold is for the extended Hilbert space to be a product state with the system Q, i.e., $\rho^{QE} = \rho^Q \otimes \rho^E$ [60,61]. This condition is reflected in Eqs. (6) and (7) where each unitary operation U_1 and U_2 acts on the product states $\rho_0^Q \otimes \rho^E$ and $\rho_1^Q \otimes \rho^N$. Hence, two extended systems E and N that are initially uncorrelated with Q are required, one for each CPTP map Φ_1 and Φ_2 as shown in Fig. 1(a).

On the other hand, if we limit the system to a single environment E such that both U_1 and U_2 act on $\mathcal{H}^Q \otimes \mathcal{H}^E$ as shown in Fig. 1(b), we have

$$\Phi_1(\rho_0^Q) = \rho_1^Q = \mathrm{Tr}_E[U_1(\rho_0^Q \otimes \rho^E)U_1^\dagger], \qquad (9)$$

$$\Phi_2(\rho_1^Q) \neq \Gamma(\rho_1^Q) = \rho_2^Q = \mathrm{Tr}_E[U_2(\rho_1^{QE})U_2^\dagger], \qquad (10)$$

where $\rho_1^{QE} = U_1(\rho_0^Q \otimes \rho^E)U_1^\dagger$, and Γ is not a valid CPTP operation. Since ρ_1^{QE} is not a product state in general, there is no CPTP map Φ_2 that can map ρ_1^Q to ρ_2^Q in general. Thus, the CPTP map Φ describing the evolution of $\rho_0^Q \to \rho_2^Q$,

$$\Phi(\rho_0^Q) = \rho_2^Q = \mathrm{Tr}_E[U_2 U_1(\rho_0^Q \otimes \rho^E)U_1^\dagger U_2^\dagger], \qquad (11)$$

is CP indivisible between the time step of the operation of U_2 with $\Phi \neq \Phi_2 \circ \Phi_1$. This correlation between the environment E and system Q, where it is nonseparable into a product state, is precisely the memory in the system that leads to its indivisibility and thus non-Markovianity. For the process to be Markovian, the environment must be memoryless such that it is a product state with system Q at every time step [40]. The non-Markovianity implies that the monotonicity of the coherent information can be violated after the operation of U_2 with

$$I_c(\rho_2^Q) \overset{\leqslant}{\underset{\geqslant}{}} I_c(\rho_1^Q) \leqslant I_c(\rho_0^Q), \qquad (12)$$

where there can be possible information revival for $I_c(\rho_2^Q)$.

The two cases can be generalized by a unitary $U_N \in \mathcal{H}^N \otimes \mathcal{H}^E$ acting on the extended systems N and E as shown in Fig. 1(c). If $U_N = \mathrm{SWAP}$, we obtain the Markovian case where U_1 and U_2 act on different environments E and N that are initially uncorrelated to Q. If $U_N = I \otimes I$, where I is the identity operation, we obtain the non-Markovian case where both U_1 and U_2 act on the same environment E. The operation of U_N can be thought of as some kind of information scrambling in the environment, possibly characterized by an out-of-time ordered correlator to describe the spreading of information from E to N [62]. For example, U_N might be time dependent such that in very short timescales we have $U_N \approx I \otimes I$, but for a long time interval it approaches $U_N \approx \mathrm{SWAP}$, as the environment equilibrates over time [63]. However, for
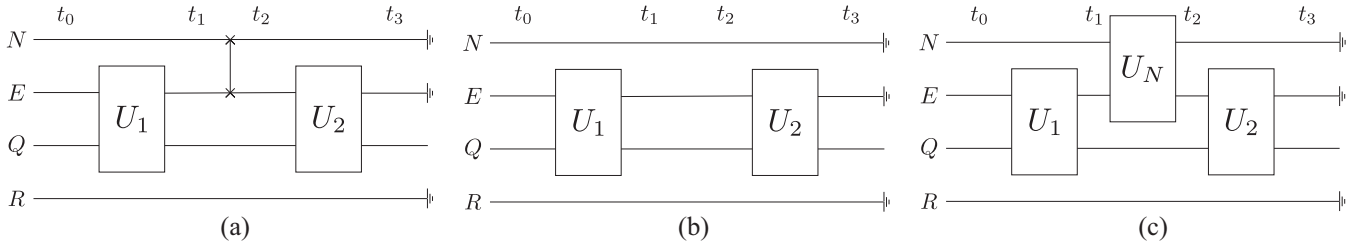
FIG. 1. (a) A single-pass circuit that is fully Markovian with U_1 and U_2 acting on different environments E and N, which are initially uncorrelated with Q. This is achieved with a SWAP operation on E and N before the operation of U_2. (b) A different single-pass circuit that exhibits non-Markovian effects with U_1 and U_2 acting on the same environment E. Non-Markovian effects manifest as the violation of the information monotone, where there can be revival of information after the operation of U_2. (c) A single-pass circuit that generalizes (a) and (b) by having its non-Markovianity controlled by the operation U_N. The (a) case is achieved for $U_N = $ SWAP, and the (b) case is achieved for $U_N = I \otimes I$. The reference system R is also included which purifies the initial state in Q into $|QR\rangle$. It should be noted that only system Q is accessible to a receiver at the end of the circuit, for which a general decoding operation can be performed, which is not shown in the diagram. Inaccessible systems are terminated with a ground symbol.

our purposes we will simply choose U_N based on its entangling capability as will be defined in Sec. III B.

Note that if U_1 is a local unitary that acts locally, i.e., $U_1 = U_1^Q \otimes U_1^E$, then ρ_1^{QE} will remain as a product state regardless of the operation of U_N, and the divisibility condition will be fulfilled with $\Phi = \Phi_2 \circ \Phi_1$, leading to the Markovian case. As local unitary operations are nonentangling, this hints at the interplay between entangling dynamics, non-Markovianity, and the transmission of information, as will be explored in Sec. III. While there are many choices of information monotones to determine the presence of non-Markovianity, this interplay of entanglement dynamics and non-Markovianity leads us to focus on the entanglement monotone $\mathsf{E}(\rho^{QR})$ between the information-carrying system Q and a reference system R. The revival of this entanglement monotone in a non-Markovian process was explored by Rivas, Huelga, and Plenio (RHP) in Ref. [51], and its monotonic nature is due to the fact that entanglement cannot increase under the local operation and classical communication (LOCC) of $\Phi^Q \otimes I^R$. Therefore, a revival of $\mathsf{E}(\rho^{QR})$ implies that Φ^Q is not completely positive, and thus does not fulfill the divisibility property.

C. Communication capacities and entanglement monotone

We are concerned with the transmission of information in our system, as well as the quantum switch's enhancement of it. Particularly, the quantum switch was shown to enhance the classical and quantum capacities [23–28], which are defined by the Holevo quantity and the coherent information. Here, we define these quantities and describe how their revival in a non-Markovian system corresponds to the revival of the entanglement monotone.

A typical communication protocol is shown in Fig. 2 where Alice would like to transmit some information to Bob who is in a different laboratory. Alice will encode this information via an encoding operation $\mathcal{E}$ into an information-carrying quantum state ρ^Q in system Q, with a reference state R that purifies Q into $|QR\rangle$, such that systems Q and R are entangled. Alice then sends the state ρ^Q through a quantum communication channel Φ that has an environmental representation of $\Phi(\rho^Q) = \rho^{Q'} = \text{Tr}_E[U(\rho^E \otimes \rho^Q)U^\dagger]$ to Bob. Bob then performs a general decoding operation $\mathcal{D}$ on the received state

$\rho^{Q'}$ to recover the information that Alice sent which is stored in system B.

The classical capacity [6,7] of a single use of the channel Φ, referred to as the one-shot classical capacity $\chi(\Phi)$, is

$$\chi(\Phi) = \max_{\{p_a, \rho_a^Q\}} \chi(\rho^Q, \Phi), \tag{13}$$

where

$$\chi(\rho^Q, \Phi) = S(\Phi(\rho^Q)) - \sum_a p_a S(\Phi(\rho_a^Q)) \tag{14}$$

is known as the Holevo quantity, and $\rho^Q = \sum_a p_a \rho_a^Q$ is the state that Alice encoded. The maximization for the one-shot capacity was shown to suffice for pure states of $\{\rho_a^Q\}$.

In the case of repeated use of the channel, i.e., Alice and Bob can decide to transmit information by repeated use of the channel Φ, where Alice encodes the state $|Q^{\otimes n}R\rangle \in \mathcal{H}^{Q^{\otimes n}} \otimes \mathcal{H}^R$ and sends the n systems $Q^{\otimes n}$ through n uses of the channel $\Phi^{\otimes n}$ to Bob, who then performs the decoding operation $\mathcal{D}: Q^{\otimes n} \to B$. In this case, Alice could prepare product state inputs that are independent to each other for every use of the channel, or she can prepare input states that are entangled across different uses of the channel. Similarly, Bob can perform independent measurements on each output of the different uses of the channel for his decoding operation, or he can perform a joint measurement on the outputs of all the different uses. The general form of the asymptotic classical capacity over repeated use of the channel that includes these
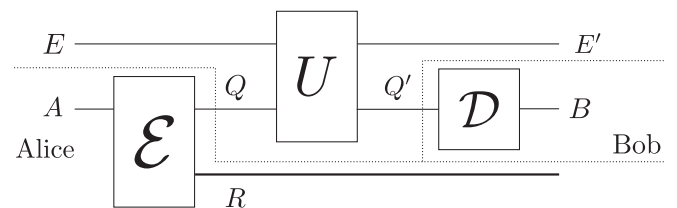

FIG. 2. A typical communication protocol where Alice encodes her information into a bipartite-entangled state $|QR\rangle$ with an encoding operation $\mathcal{E}: A \to Q \otimes R$ and send system Q through a channel with unitary $U: E \otimes Q \to E' \otimes Q'$ to Bob, who then perform a general decoding operation $\mathcal{D}: Q' \to B$.

cases is

$$C(\Phi) = \lim_{n \to \infty} \frac{1}{n} \chi(\Phi^{\otimes n}), \tag{15}$$

where $\chi(\Phi^{\otimes n})$ is the one-shot classical capacity of n parallel channels Φ.

Moving on to the case of quantum information [5,8,9], we require the coherent information I_c which is defined as the difference between the von Neumann entropies of the output of the channel Q' and the resulting environment E':

$$\begin{aligned} I_c(\rho^Q, \Phi) &= S(\rho^{Q'}) - S(\rho^{E'}) \\ &= S(\Phi(\rho^Q)) - S(\widetilde{\Phi}(\rho^Q)), \tag{16} \end{aligned}$$

where in the last equality we defined the complementary map $\widetilde{\Phi}$ such that $\widetilde{\Phi}(\rho^Q) = \rho^{E'} = \mathrm{Tr}_Q[U(\rho^E \otimes \rho^Q)U^\dagger]$. Similar to the Holevo quantity, the one-shot quantum capacity is

$$I_c(\Phi) = \max_{\{p_a, \rho_a^Q\}} I_c(\rho^Q, \Phi), \tag{17}$$

and the asymptotic quantum capacity over repeated use of the channel is

$$Q(\Phi) = \lim_{n \to \infty} \frac{1}{n} I_c(\Phi^{\otimes n}), \tag{18}$$

where $I_c(\Phi^{\otimes n})$ is the one-shot quantum capacity of n parallel channels Φ. It should also be noted that the coherent information and Holevo quantity are closely related:

$$\begin{aligned} I_c(\rho^Q, \Phi) &= S(\Phi(\rho^Q)) - S(\widetilde{\Phi}(\rho^Q)) \\ &\quad - \sum_a p_a S(\Phi(\rho_a^Q)) + \sum_a p_a S(\widetilde{\Phi}(\rho_a^Q)) \\ &= \chi(\rho^Q, \Phi) - \chi(\rho^Q, \widetilde{\Phi}), \tag{19} \end{aligned}$$

where in the first equality we note that $S(\Phi(\rho_a^Q)) = S(\widetilde{\Phi}(\rho_a^Q))$ for all a. Therefore, the coherent information can also be thought of as how much more classical information Bob has as compared to those lost to the environment.

For the coherent information to take the maximum value, we need $S(\rho^{E'})$ to be as small as possible while $S(\rho^{Q'})$ as large as possible according to Eq. (16). Since the joint state $\rho^{E'Q'R}$ is pure, this happens when $S(\rho^{E'}) = S(\rho^{Q'R}) = 0$ which implies that the system $Q'R$ is in a pure state. $S(\rho^{Q'})$ then takes the largest value when the systems Q' and R are maximally entangled. Therefore, the transmission of quantum information can also be thought of as the preservation of the initial entanglement between Q and R or, in other words, the generation of entanglement between Alice and Bob via the joint state $\rho^{Q'R}$. Indeed, it was shown by Devetak in Ref. [9] that the asymptotic quantum capacity $Q(\Phi)$ is equal to the asymptotic entanglement generation capacity between Alice and Bob. Alternatively, this preservation of the entanglement between Q and R was also defined as the entanglement fidelity, which is the state fidelity of the input and output states $|QR\rangle$ and $\rho^{Q'R}$ [3,5]. If the channel is ideally noiseless, then the entanglement fidelity is unity and the initial entanglement of $|QR\rangle$ is perfectly preserved with $|Q'R\rangle = |QR\rangle$.

It was also shown that the classical information $J_{RE'}^{\leftarrow}$ that one can obtain about system R via a measurement on environment E' has an inverse relation with the entanglement of $\rho^{Q'R}$ with $d\mathsf{E}(\rho^{Q'R})/dt = -dJ_{RE'}^{\leftarrow}/dt$ where the entanglement

measure E (not to be confused with environment E) is chosen to be the entanglement of formation (EoF) [64]. For a continuous Markovian process, we expect the entanglement monotone to be decreasing with $d\mathsf{E}(\rho^{Q'R})/dt < 0$, and thus $dJ_{RE'}^{\leftarrow}/dt > 0$ for all t, which reflects the flow of classical information away from Q to E'. On the other hand, for a non-Markovian process with a revival of the entanglement monotone, we have $d\mathsf{E}(\rho^{Q'R})/dt > 0$, and thus $dJ_{RE'}^{\leftarrow}/dt < 0$ for some t where the classical information flows back into the information-carrying system Q'.

Ultimately, the capacity to transmit information between two parties is dependent on the capacity to transmit or generate entanglement between the two parties, and similar to the measure $d\mathsf{E}(\rho^{Q'R})/dt$ in Ref. [64], in our discrete time case we are concerned with the change of the entanglement monotone $\Delta\mathsf{E}(\rho^{QR}) = \mathsf{E}(\rho_{t+1}^{QR}) - \mathsf{E}(\rho_t^{QR})$ at every time step. $\Delta\mathsf{E}(\rho^{QR}) \geqslant 0$ would imply the presence of non-Markovianity and allows the possibility for a revival of the coherent information and Holevo quantity, which can correspond to a revival of the quantum and classical capacities. However, it should be noted that the presence of revival is dependent on the choice of entanglement measure E, e.g., revival can be present for one choice of measure, but absent in another. Nevertheless, for a Markovian process, we expect no revival for any and all valid choices of E. On the other hand, if we can find a single valid choice of E that is nonmonotonic such that a revival is observed, then we can be sure that the process is non-Markovian in the interval of the revival [51].

III. ENTANGLING DYNAMICS

It should be noted that the change in the entanglement monotone $\mathsf{E}(\rho^{QR})$ is due to the creation or destruction of entanglement with the environment E, which is defined by its maximum change maximized over all input states, and was shown to upper bound the bidirectional communication rates between them [65,66], i.e., the greater the entanglement creation or destruction, the greater the amount of information flows between the information-carrying system and the environment. Due to the monogamous nature of entanglement, this creation and destruction of entanglement can be seen as a flow or redistribution of entanglement. Therefore, the dynamics of the revival of information due to non-Markovianity can be defined as this flow of entanglement between all involving parties. In this section, we define this entanglement flow and review the definitions for the capability of a bipartite unitary to create or destroy entanglement, before applying to the single-pass circuit in Fig. 1(c) as an example.

A. Entanglement flow

A qubit A being maximally entangled with a qubit B cannot be maximally entangled with another qubit C without destroying its entanglement with B. In a sense, the entanglement that a system can share with other systems is limited [67]. This is referred to as the monogamous nature of entanglement, and is usually expressed as an inequality called the monogamy relation

$$\mathsf{E}^\alpha(\rho^{A|BC}) \geqslant \mathsf{E}^\alpha(\rho^{A|B}) + \mathsf{E}^\alpha(\rho^{A|C}), \tag{20}$$

where α is an exponent, and $\mathsf{E}(\rho^{X|Y})$ is an entanglement measure of the bipartite split of parties X and Y for the state ρ^{XY}. For conciseness, we refer to this as the bipartite split $X|Y$. Also note that the entanglement of the bipartite split is symmetric such that $\mathsf{E}(\rho^{X|Y}) = \mathsf{E}(\rho^{Y|X})$.

The choice of E and α that fulfills the monogamy relation is dependent on the dimensions of the system $d_A \otimes d_B \otimes d_C$ [68]. The first of which was shown by Coffman, Kundu, and Wooters [67], and is referred to as the CKW inequality where $d_A = d_B = d_C = 2$ and E^α is taken to be concurrence squared C^2. The CKW inequality was later extended for dimensions of $2^{\otimes n}$ systems for arbitrary n [69].

Equation (20) can be applied recursively for a state of more than three parties. For example,

$$\mathsf{E}^\alpha(\rho^{A|B(CD)}) \geqslant \mathsf{E}^\alpha(\rho^{A|B}) + \mathsf{E}^\alpha(\rho^{A|CD})$$
$$\geqslant \mathsf{E}^\alpha(\rho^{A|B}) + \mathsf{E}^\alpha(\rho^{A|C}) + \mathsf{E}^\alpha(\rho^{A|D}), \quad (21)$$

where in the first inequality we applied Eq. (20) on $\mathsf{E}^\alpha(\rho^{A|B(CD)})$ by grouping parties C and D, and making the substitution $C \to CD$. Then, in the second inequality we applied Eq. (20) again for $\mathsf{E}^\alpha(\rho^{A|CD})$.

Note, however, that $\rho^{A|CD}$ is a mixed state in general, and if $\rho^{A|B(CD)}$ is a pure state, we require the choice of measure E to be monogamous for both pure and mixed states for Eq. (21) to hold. For any measure E, we can define its associated entanglement of formation (EoF) E_f via a convex roof extension,

$$\mathsf{E}_f(\rho^{A|B}) = \min_{\{p_i, |\psi_i\rangle\}} \sum_i p_i \mathsf{E}(|\psi_i\rangle\langle\psi_i|^{A|B}), \quad (22)$$

where the minimization is taken over all pure state decompositions of $\rho^{A|B} = \sum_i p_i |\psi_i\rangle\langle\psi_i|^{A|B}$. It was shown that if E_f is monogamous for tripartite pure states, then it is also monogamous for tripartite mixed states [68]. Therefore, Eq. (21) holds for E_f, but will only hold for E if $\mathsf{E}(\rho^{A|B}) = \mathsf{E}_f(\rho^{A|B})$. This is trivially true if $\rho^{A|B}$ is pure, but for mixed states it is only true for certain measures such as concurrence squared.

To see how the monogamy relation is useful for describing the flow of entanglement under bipartite unitaries, we require a few properties of entanglement. First, we note that if

$$\rho^{A'B'C'} = (U^A \otimes U^{BC})\rho^{ABC}(U^A \otimes U^{BC})^\dagger, \quad (23)$$

then

$$\mathsf{E}(\rho^{A|BC}) = \mathsf{E}(\rho^{A'|B'C'}), \quad (24)$$

as entanglement is invariant under local unitaries. For simplicity, we will write $\rho_t^{A|BC}$ with a subscript t to define the state $\rho^{A|BC}$ at different time steps, while keeping the Hilbert space labels A, B, C unchanged.

We also define the residual entanglement as the difference between both sides of the monogamy relation in Eq. (20) with

$$\mathsf{E}^\alpha(\rho^{A|\text{res}}) = \mathsf{E}^\alpha(\rho^{A|BC}) - \mathsf{E}^\alpha(\rho^{A|B}) - \mathsf{E}^\alpha(\rho^{A|C}). \quad (25)$$

The residual entanglement accounts for all the multipartite entanglements that are not bipartite entanglements. Note that similar to Eq. (20), Eqs. (24) and (25) also extend to more than three parties.

Now, suppose we prepared an information-carrying mixed state $\rho^Q \in \mathcal{H}^Q$ that is purified as $\rho^{QR} = |QR\rangle\langle QR| \in \mathcal{H}^Q \otimes \mathcal{H}^R$,

and we interact it unitarily with an environment state $\rho^E \in \mathcal{H}^E$ by a unitary at time t, $U_t \in \mathcal{H}^E \otimes \mathcal{H}^Q$, such that

$$\rho_t^{EQR} = (U_t \otimes I)\rho_{t-1}^{EQR}(U_t \otimes I)^\dagger, \quad (26)$$

we have

$$\mathsf{E}^\alpha(\rho_t^{R|QE}) = \mathsf{E}^\alpha(\rho_{t-1}^{R|QE}),$$
$$\mathsf{E}^\alpha(\rho_t^{R|Q}) + \mathsf{E}^\alpha(\rho_t^{R|E}) + \mathsf{E}^\alpha(\rho_t^{R|\text{res}}) = \mathsf{E}^\alpha(\rho_{t-1}^{R|Q}) + \mathsf{E}^\alpha(\rho_{t-1}^{R|E})$$
$$+ \mathsf{E}^\alpha(\rho_{t-1}^{R|\text{res}}),$$
$$\Delta_t\mathsf{E}^\alpha(\rho^{R|Q}) = -\Delta_t\mathsf{E}^\alpha(\rho^{R|E})$$
$$- \Delta_t\mathsf{E}^\alpha(\rho^{R|\text{res}}), \quad (27)$$

for all time steps t. In the first and second equalities, we applied Eqs. (24) and (25), respectively, and in the third equality we have defined

$$\Delta_t\mathsf{E}^\alpha(\rho) = \mathsf{E}^\alpha(\rho_t) - \mathsf{E}^\alpha(\rho_{t-1}). \quad (28)$$

The bipartite entanglement of $R|Q$ at the left-hand side is the entanglement monotone that we are concerned with.

Not only does Eq. (27) tell us that such an interaction redistributes entanglement between $R|Q$, $R|E$, as well as the multipartite entanglement $\mathsf{E}^\alpha(\rho^{R|\text{res}})$, it also captures non-Markovian effects via the revival of the entanglement monotone of $R|Q$ where any revival must correspond to a decrease in the entanglement of $R|E$ and the multipartite residual entanglement. For the case of $t - 1 = 0$ where environment E is initially uncorrelated to system Q, we have $\mathsf{E}^\alpha(\rho_0^{R|E}) = \mathsf{E}^\alpha(\rho_0^{R|\text{res}}) = 0$, and thus the initial entanglement of $R|Q$ is lost to the environment E and to the multipartite entanglement with

$$-\Delta_1\mathsf{E}^\alpha(\rho^{R|Q}) = \mathsf{E}^\alpha(\rho_1^{R|E}) + \mathsf{E}^\alpha(\rho_1^{R|\text{res}}). \quad (29)$$

This is as expected for a Markovian process where the entanglement monotone must decrease, which corresponds to a flow of information away from the information-carrying system.

Furthermore, we note that the operation of U_t can also create or destroy bipartite entanglements between $Q|E$, which is dependent on its entangling capability as well as the presence of initial entanglement. Since we also have

$$\mathsf{E}^\alpha(\rho^{Q|RE}) = \mathsf{E}^\alpha(\rho^{Q|R}) + \mathsf{E}^\alpha(\rho^{Q|E}) + \mathsf{E}^\alpha(\rho^{Q|\text{res}}), \quad (30)$$

thus,

$$\Delta_t\mathsf{E}^\alpha(\rho^{R|Q}) = \Delta_t\mathsf{E}^\alpha(\rho^{Q|RE}) - \Delta_t\mathsf{E}^\alpha(\rho^{Q|E}) - \Delta_t\mathsf{E}^\alpha(\rho^{Q|\text{res}}). \quad (31)$$

Now it is also clear that there is direct entanglement flow between $R|Q$ and $Q|E$, in accord with Refs. [65,66] where the entangling capability of a bipartite unitary, which creates or destroys entanglement between $Q|E$, upper bounds the bidirectional communication of the two entangling parties, which corresponds to a decrease or revival of the entanglement monotone of $R|Q$.

B. Entangling capability of bipartite unitaries

As we expect entanglement generation, destruction, or flow to depend on the entangling capability of the channel's

bipartite unitary in the environmental representation, here, we will give a brief review of the entangling capability of bipartite unitaries which will lead us to the form of unitary that we use in our numerical results in later sections. While there are many measures of the entangling capability or entangling strength of quantum operations [70–72], their differences and applications are unimportant for our purposes, and we will take the measures defined in Ref. [73], which focus on the maximum possible entanglement generation. This family of measures for the entangling capability of unitaries are denoted with $K(U)$, and should not be confused with the family of measures for the entanglement of states which are denoted with $\mathsf{E}(\rho)$ as discussed in previous sections.

The capability of a bipartite unitary $U^{AB} \in \mathcal{H}^A \otimes \mathcal{H}^B$ to create or destroy bipartite entanglement can be quantified by the maximum change in entanglement it is capable of,

$$K_{\Delta \mathsf{E}}(U^{AB}) = \sup_{|\psi\rangle} |\mathsf{E}(U^{AB}|\psi\rangle) - \mathsf{E}(|\psi\rangle)|, \quad (32)$$

where the supremum is taken over all $|\psi\rangle = |AR_A BR_B\rangle$ where R_A and R_B are purification states of A and B, respectively. If there is no initial entanglement between systems A and B, we have $K_{\Delta \mathsf{E}} = K_{\mathsf{E}}$ where K_{E} is called the entangling power,

$$K_{\mathsf{E}}(U^{AB}) = \max_{\{|AR_A\rangle, |BR_B\rangle\}} \mathsf{E}(U^{AB}|AR_A\rangle|BR_B\rangle), \quad (33)$$

otherwise we have $K_{\mathsf{E}} \leqslant K_{\Delta \mathsf{E}}$ in general.

It was shown that an arbitrary bipartite unitary $W^{AB} \in \mathcal{H}^A \otimes \mathcal{H}^B$ can be decomposed into

$$W^{AB} = (U^A \otimes U^B)U^{AB}(V^A \otimes V^B), \quad (34)$$

where U^A, U^B, V^A, and V^B are local unitaries, while U^{AB} is a bipartite unitary that is diagonal in the magic basis [70]. Since entanglement is invariant under local unitary operations, we have $K(W^{AB}) = K(U^{AB})$, and we say that W^{AB} is locally equivalent to U^{AB} under local unitaries. U^{AB} can be expressed in its operator Schmidt form of

$$U^{AB} = \sum_i c_i A_i \otimes B_i, \quad (35)$$

where the sets of operators $\{A_i\}$ and $\{B_i\}$ are orthonormal under the Hilbert-Schmidt inner product in their respective subspaces, and $\sum_i |c_i|^2 = 1$. The number of nonzero c_i is referred to as the Schmidt rank of U^{AB}. For the case of qubits with $d_A = d_B = 2$, up to local unitaries, U^{AB} can be expressed in the canonical form of

$$U^{AB} = c_0 I \otimes I + c_1 X \otimes X + c_2 Y \otimes Y + c_3 Z \otimes Z, \quad (36)$$

where I, X, Y, Z are the identity and Pauli matrices.

The Schmidt strength is defined as the Shannon entropy of the normalized c_i^2:

$$K_{\text{sch}}(U^{AB}) = H\left(\left\{\frac{c_i^2}{d_A d_B}\right\}\right). \quad (37)$$

For the identity operator, we have $K_{\text{sch}} = 0$, and for the SWAP gate we have a maximum of $K_{\text{sch}} = 2$. In general, we have $K_{\text{sch}}(U^{AB}) \leqslant K_{\mathsf{E}}(U^{AB}) \leqslant K_{\Delta E}(U^{AB})$, and $K_{\text{sch}}(U^{AB}) = K_{\mathsf{E}}(U^{AB})$ if U^{AB} has Schmidt rank $\leqslant 2$.

While there are closed-form solutions of K_{E} and $K_{\Delta E}$ for specific cases [74], in general the maximization is difficult to

compute. For our purposes, we will use a more constrained form of Eq. (36) of

$$\begin{aligned} U_q &= \left(\sqrt{1-q}I \otimes I + i\sqrt{q}X \otimes X\right) \\ &\quad \times \left(\sqrt{1-q}I \otimes I + i\sqrt{q}Z \otimes Z\right) \\ &= (1-q)I \otimes I + i\sqrt{q(1-q)}X \otimes X \\ &\quad - qY \otimes Y + i\sqrt{q(1-q)}Z \otimes Z, \end{aligned} \quad (38)$$

where we have a local unitary of $K_{\text{sch}}(U_q) = 0$ when $q = 0, 1$, and a maximum entangling capability of $K_{\text{sch}}(U_Q) = 2$ when $q = 0.5$. The advantages of U_q are that its Schmidt coefficients depend only on a single variable $0 \leqslant q \leqslant 1$, and that it was shown numerically that for the range of $0.1 \lesssim q \lesssim 0.9$ where $K_{\text{sch}}(U_q) \geqslant 1$, we have $K_{\text{sch}}(U_q) = K_{\mathsf{E}}(U_q)$ [73].

C. Example: Single pass

As an example, we will demonstrate how the entangling capabilities of U_1, U_2, and U_N can lead to non-Markovian effects of entanglement monotone revival for the single-pass circuit in Fig. 1(c).

First, we note that systems E and N are initially pure and uncorrelated with systems Q, R, and each other. Therefore, under the operation of U_1 in $t_0 \rightarrow t_1$, the bipartite entanglement of $R|Q$ must decrease as it is a Markovian process:

$$\mathsf{E}^\alpha(\rho_0^{R|NEQ}) = \mathsf{E}^\alpha(\rho_1^{R|NEQ}),$$
$$\mathsf{E}^\alpha(\rho_0^{R|Q}) = \mathsf{E}^\alpha(\rho_1^{R|E}) + \mathsf{E}^\alpha(\rho_1^{R|Q}) + \mathsf{E}^\alpha(\rho_1^{R|\text{res}}),$$
$$\Delta_1 \mathsf{E}^\alpha(\rho^{R|Q}) = -\mathsf{E}^\alpha(\rho_1^{R|E}) - \mathsf{E}^\alpha(\rho_1^{R|\text{res}}), \quad (39)$$

where we have simply applied Eq. (27). In the first equality we have Eq. (24), where the entanglements of $\rho_0^{R|NEQ}$ and $\rho_1^{R|NEQ}$ are invariant as U_1 acts locally for the bipartite split of $R|NEQ$. In the second equality, on the left-hand side we note that only systems R and Q are entangled at $t = 0$, and on the right-hand side we applied Eq. (25), noting that $\mathsf{E}(\rho_1^{R|N}) = 0$. Since entanglement measures must be positive, the right-hand side is negative and thus $\Delta_1 \mathsf{E}^\alpha(\rho^{R|Q}) \leqslant 0$, as entanglement flows to the environment and multipartite entanglement. Next, since $\rho_1^{RQ} = \rho_2^{RQ}$, we have $\mathsf{E}^\alpha(\rho_1^{R|Q}) = \mathsf{E}^\alpha(\rho_2^{R|Q})$. Then, the operation of U_N in $t_1 \rightarrow t_2$ simply redistributes the bipartite entanglements of system E:

$$\mathsf{E}^\alpha(\rho_1^{Q|NER}) = \mathsf{E}^\alpha(\rho_2^{Q|NER}),$$
$$\mathsf{E}^\alpha(\rho_1^{Q|E}) + \mathsf{E}^\alpha(\rho_1^{Q|\text{res}}) = \mathsf{E}^\alpha(\rho_2^{Q|N}) + \mathsf{E}^\alpha(\rho_2^{Q|E}) + \mathsf{E}^\alpha(\rho_2^{Q|\text{res}}),$$
$$\Delta_2 \mathsf{E}^\alpha(\rho^{Q|E}) = -\mathsf{E}^\alpha(\rho_2^{Q|N}) - \Delta_2 \mathsf{E}^\alpha(\rho^{Q|\text{res}}), \quad (40)$$

where again we applied Eqs. (24) and (25) noting that $\mathsf{E}(\rho_1^{Q|N}) = 0$ as systems Q and N are uncorrelated before the operation of U_N. Similarly,

$$\mathsf{E}^\alpha(\rho_1^{R|NEQ}) = \mathsf{E}^\alpha(\rho_2^{R|NEQ}),$$
$$\mathsf{E}^\alpha(\rho_1^{R|E}) + \mathsf{E}^\alpha(\rho_1^{R|\text{res}}) = \mathsf{E}^\alpha(\rho_2^{R|N}) + \mathsf{E}^\alpha(\rho_2^{R|E}) + \mathsf{E}^\alpha(\rho_2^{R|\text{res}}),$$
$$\Delta_2 \mathsf{E}^\alpha(\rho^{R|E}) = -\mathsf{E}^\alpha(\rho_2^{R|N}) - \Delta_2 \mathsf{E}^\alpha(\rho^{R|\text{res}}). \quad (41)$$

As system N is initially uncorrelated with systems Q and R, interacting systems E and N with U_N cannot

increase the bipartite entanglements of $Q|E$ and $R|E$. Therefore, $\Delta_2 \mathsf{E}^\alpha(\rho^{Q|E}) \leqslant 0$ and $\Delta_2 \mathsf{E}^\alpha(\rho^{R|E}) \leqslant 0$. As seen in Eqs. (27) and (31), any revival of the entanglement monotone must come from the bipartite entanglement of $Q|E$, $R|E$, and multipartite entanglement. Therefore, here we see that

the operation of U_N will reduce this revival as the bipartite entanglements of $Q|E$ and $R|E$ are reduced after the operation of U_N.

Finally, for the operation of U_2 in $t_2 \to t_3$, we note that $\rho_2^{RN} = \rho_3^{RN}$, and thus

$$\mathsf{E}^\alpha(\rho_2^{R|NEQ}) = \mathsf{E}^\alpha(\rho_3^{R|NEQ}),$$
$$\mathsf{E}^\alpha(\rho_2^{R|E}) + \mathsf{E}^\alpha(\rho_2^{R|Q}) + \mathsf{E}^\alpha(\rho_2^{R|\mathrm{res}}) = \mathsf{E}^\alpha(\rho_3^{R|E}) + \mathsf{E}^\alpha(\rho_3^{R|Q}) + \mathsf{E}^\alpha(\rho_3^{R|\mathrm{res}}),$$
$$\Delta_3 \mathsf{E}^\alpha(\rho^{R|Q}) = -\Delta_3 \mathsf{E}^\alpha(\rho^{R|E}) - \Delta_3 \mathsf{E}^\alpha(\rho^{R|\mathrm{res}}). \tag{42}$$

Again, we see that any revival of the entanglement monotone $\mathsf{E}(\rho^{R|Q})$ must correspond to a decrease of entanglement in environment E and the multipartite entanglement $\widetilde{\mathsf{E}}^\alpha(\rho^{R|\mathrm{res}})$.

In the Markovian case in Fig. 1(a) where $U_N = \mathrm{SWAP}$, the bipartite entanglement of $R|E$ is completely destroyed with $\mathsf{E}^\alpha(\rho_2^{R|E}) = 0$ and thus $\mathsf{E}^\alpha(\rho_2^{R|EQ}) = \mathsf{E}^\alpha(\rho_2^{R|Q})$. Applying the monogamy relation for the mixed state $\rho^{R|EQ}$,

$$\mathsf{E}^\alpha(\rho_2^{R|EQ}) = \mathsf{E}^\alpha(\rho_3^{R|EQ}),$$
$$\mathsf{E}^\alpha(\rho_2^{R|Q}) = \mathsf{E}^\alpha(\rho_3^{R|E}) + \mathsf{E}^\alpha(\rho_3^{R|Q}) + \widetilde{\mathsf{E}}^\alpha(\rho_3^{R|\mathrm{res}}),$$
$$\Delta_3 \mathsf{E}^\alpha(\rho^{R|Q}) = -\mathsf{E}^\alpha(\rho_3^{R|E}) - \widetilde{\mathsf{E}}^\alpha(\rho_3^{R|\mathrm{res}}), \tag{43}$$

where

$$\widetilde{\mathsf{E}}^\alpha(\rho_3^{R|\mathrm{res}}) = \mathsf{E}^\alpha(\rho_3^{R|EQ}) - \mathsf{E}^\alpha(\rho_3^{R|E}) - \mathsf{E}^\alpha(\rho_3^{R|Q}), \tag{44}$$

in contrast to Eq. (42) where we have

$$\mathsf{E}^\alpha(\rho_3^{R|\mathrm{res}}) = \mathsf{E}^\alpha(\rho_3^{R|NEQ}) - \mathsf{E}^\alpha(\rho_3^{R|N})$$
$$- \mathsf{E}^\alpha(\rho_3^{R|E}) - \mathsf{E}^\alpha(\rho_3^{R|Q}). \tag{45}$$

In general, $\widetilde{\mathsf{E}}^\alpha(\rho_3^{R|\mathrm{res}}) \neq \mathsf{E}^\alpha(\rho_3^{R|\mathrm{res}})$. Therefore, we see that the entanglement monotone of $\mathsf{E}(\rho^{R|Q})$ must decrease after the operation of U_2 as expected of a Markovian operation. We note that Eq. (43) is true whenever U_N is maximally entangling, i.e., $K_{\mathrm{sch}}(U_N) = 2$.

The amount of revival in Eq. (42) is dependent on the entangling capabilities of U_1, U_2, and U_N. Naturally, as the entangling capability of U_N increases, we expect the amount of information revival to decrease as the system approaches a Markovian system. If U_1 is a highly entangling operation such that information is lost as there is a large flow of the entanglement monotone to the environment and multipartite entanglement, then we expect U_2 to enable revival even if it is weakly entangling. On the other hand, if U_1 is weakly entangling such that almost all information remains in system Q as the entanglement monotone is largely preserved, then we expect that U_2 can easily displace information away from Q with a decrease in the entanglement monotone, and is unable to grant a large revival if any. We will demonstrate the relation between entangling capabilities and revival to the entanglement monotone numerically.

For the single-pass case in Fig. 1(c), we have a system of $d_N \otimes d_E \otimes d_Q \otimes d_R = 2^{\otimes 4}$ for which the extended CKW monogamy inequality for concurrence squared holds [69]. Therefore, we can choose concurrence squared as our entan-

glement measure with $\mathsf{E}^\alpha \to C^2$. Our entanglement monotone is thus the concurrence squared of the bipartite split of $R|Q$, $C^2(\rho^{R|Q})$.

For simplicity, we prepare the information-carrying system Q as follows:

$$\rho_0^Q = p|0\rangle\langle 0| + (1-p)|1\rangle\langle 1|, \tag{46}$$

with $\rho_0^E = \rho_0^N = |0\rangle\langle 0|$. For U_1, U_2, and U_N, they will take the form of U_q in Eq. (38), where we denote their corresponding variable q as q_1, q_2, and n, respectively. Again, we note that as we are only concerned with the changes in entanglement of the system, it will suffice to consider unitaries in the canonical form of Eq. (36), and U_q covers the entire range of Schmidt strengths of $0 \leqslant K_{\mathrm{sch}}(U_q) \leqslant 2$. While we have taken the unitaries to be in the form of U_q here for the numerical computation, we emphasize that the equations for entanglement flow are general for all unitaries.

In Fig. 3, for the operation of U_1 from time step $t_0 \to t_1$, we see that indeed the change in concurrence squared $\Delta_1 C^2(\rho^{R|Q})$ of the bipartite split of $R|Q$ is negative of the change in concurrence squared $\Delta_1 C^2(\rho^{R|E})$ of the bipartite split $R|E$, and of the change in residual $\Delta_1 C^2(\rho^{R|\mathrm{res}})$, as shown in Eq. (39). The amount of flow of entanglement from $R|Q$ to $R|E$ and multipartite entanglement is dependent on the entangling power $K_{\mathsf{E}}(U_1)$ of U_1 which is equal to its Schmidt strength $K_{\mathrm{sch}}(U_1)$ for $0.1 \lesssim q_1 \lesssim 0.9$ and lower bounded by it otherwise.
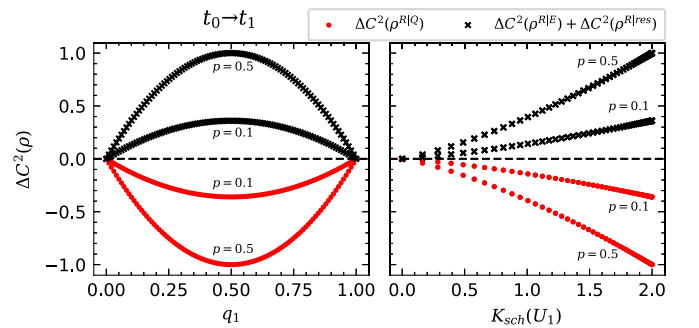

FIG. 3. Change in the entanglement monotone of concurrence squared $\Delta_1 C^2(\rho^{R|Q})$ of bipartite split $R|Q$ after the operation of U_1 from time step $t_0 \to t_1$. The decrease in $\Delta_1 C^2(\rho^{R|Q})$ is accompanied by a corresponding increase in $\Delta_1 C^2(\rho^{R|E})$ and $\Delta_1 C^2(\rho^{R|\mathrm{res}})$. The change is larger for U_1 that is more entangling, and for $p \to 0.5$ as more initial entanglement is carried in the system.
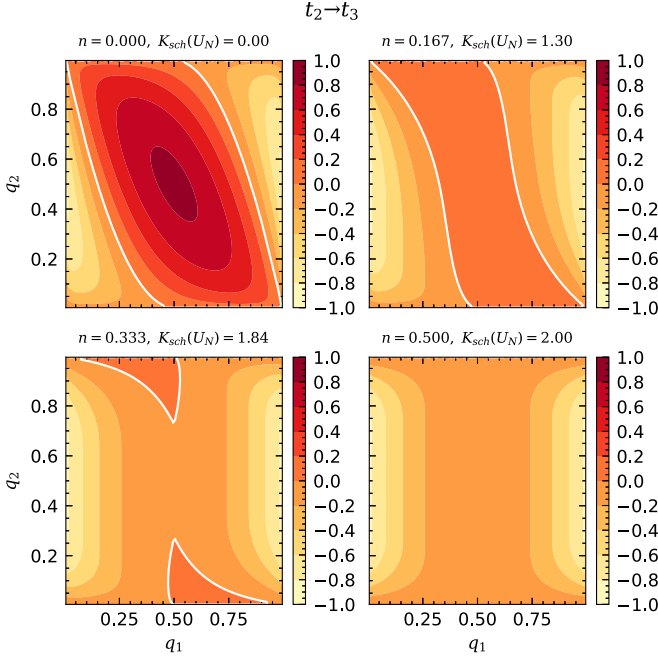
FIG. 4. The change in the entanglement monotone of concurrence squared $\Delta_3 C^2(\rho^{R|Q})$ of $R|Q$ (shown as the color map) after the operation of U_2 from time step $t_2 \rightarrow t_3$ for $p = 0.5$, and its dependence on q_1, q_2, and n. The white lines are values of q_1 and q_2 that have zero change in concurrence squared, and are the boundaries between positive and negative changes. A positive change signifies a revival of of the entanglement monotone due to non-Markovianity. As the Schmidt strength of U_N increases, the amount of revival decreases. The amount of revival is largest for $n = 0$ where $U_N = I \otimes I$, and no revival is present for $n = 0.5$ where U_N is maximally entangling as it is fully Markovian.

The amount of entanglement created or destroyed by the operation of U_2 is more complicated as it depends on the operations of U_1 and U_N. Here, demonstrating the choices of q_1 and q_2 that leads to revival or further decrease in the entanglement monotone $C^2(\rho^{R|Q})$ will suffice for our purposes, which is shown as the color map in the contour plot in Fig. 4, where the white lines are values of q_1 and q_2 that have zero change in the entanglement monotone, and thus bounds the ranges of q_1 and q_2 that give a revival of the entanglement monotone. As expected, no revival of the entanglement monotone is present for the case of $n = 0.5$ where U_N is maximally entangling as it is fully Markovian. The possible values and magnitudes for the revival also decrease as $n \rightarrow 0.5$, and are the greatest for $n = 0$ with $U_N = I \otimes I$ as the system is fully non-Markovian as in Fig. 1(b). It is also important to note that even if the system is non-Markovian in the case of $n \neq 0.5$, not all possible values of q_1 and q_2 can grant a revival. These U_1 and U_2 that do not grant a revival lead to an eternally non-Markovian system where there is no information backflow despite violating CP divisibility as described in Sec. II A [46].

IV. QUANTUM SWITCH

A. Non-Markovianity in the quantum switch

The two-party quantum switch puts two operations Φ_A and Φ_B in a controlled superposition of opposite causal orders,

$\Phi_B \circ \Phi_A$ and $\Phi_A \circ \Phi_B$, controlled by a control qubit. For example, if the control qubit is $|0\rangle$, the operation $\mathcal{F} = \Phi_B \circ \Phi_A$ is performed, but if the control qubit is $|1\rangle$, the operation $\mathcal{G} = \Phi_A \circ \Phi_B$ is performed. The environmental representation of the quantum switch is shown in Fig. 5(a) with $U_N = I \otimes I$. While such a circuit might be regarded as a 4-space-time event or 4-event quantum switch due to the presence of four operations on system Q over time, we note that this is only due to the limitations on the clarity of circuit diagrams to denote controlled operations, and that Fig. 5(a) can also represent a two-event quantum switch such as the one in Ref. [75] by treating the first two and the last two operations as a single unitary operation each. With $U_N = I \otimes I$, the circuit reduces to the quantum switch with Kraus operators of

$$K_{ij}^{\text{sw}} = |0\rangle\langle 0| \otimes B_j A_i + |1\rangle\langle 1| \otimes A_i B_j, \qquad (47)$$

acting on $\rho_0^C \otimes \rho_0^Q$ such that

$$\Phi^{\text{sw}}(\rho_0^C \otimes \rho_0^Q) = \sum_{ij} K_{ij}^{\text{sw}}(\rho_0^C \otimes \rho_0^Q) K_{ij}^{\text{sw}\dagger}, \qquad (48)$$

where Φ^{sw} is the operation of the quantum switch, and that $\{A_i\}$ and $\{B_j\}$ are the set of Kraus operators for Φ_A and Φ_B, respectively, such that $\Phi_A(\rho_0^Q) = \sum_i A_i \rho_0^Q A_i^\dagger$ and $\Phi_B(\rho_0^Q) = \sum_i B_i \rho_0^Q B_i^\dagger$. The shared indices on both paths of the superposition imply that the operations or environmental noises on both paths $\mathcal{F} = \Phi_B \circ \Phi_A$ and $\mathcal{G} = \Phi_A \circ \Phi_B$ are correlated to each other.

On the other hand, if $U_N = \text{SWAP}$ the circuit reduces to a superposition of independent trajectories where $\mathcal{F}$ and $\mathcal{G}$ are independent channels with Kraus operators of

$$K_{ijkl}^{\text{traj}} = \alpha_0 |0\rangle\langle 0| \otimes B_j A_i + \alpha_1 |1\rangle\langle 1| \otimes A_k B_l, \qquad (49)$$

where α_0 and α_1 are complex coefficients that ensure the completeness relation $\sum_{ijkl} K_{ijkl}^{\text{traj}\dagger} K_{ijkl}^{\text{traj}} = I$. Following the terminology of Ref. [34], we refer to the operation

$$\Phi^{\text{traj}}(\rho_0^C \otimes \rho_0^Q) = \sum_{ijkl} K_{ijkl}^{\text{traj}}(\rho_0^C \otimes \rho_0^Q) K_{ijkl}^{\text{traj}\dagger} \qquad (50)$$

as a superposition of trajectories in contrast with the quantum switch's superposition of causal orders in Eq. (47). We also take this opportunity to define a superposition of independent channels:

$$K_{ij}^{\text{indep}} = \beta_0 |0\rangle\langle 0| \otimes A_i + \beta_1 |1\rangle\langle 1| \otimes B_j, \qquad (51)$$

where again β_0 and β_1 are complex coefficients that ensure the completeness relation for K_{ij}^{indep}. It should be clear that the superposition of trajectories in Eq. (49) is in the form of the superposition of independent channels in Eq. (51). However, in the context of the quantum switch, we refer to a superposition of independent channels as the controlled superposition of Φ_A and Φ_B, while the superposition of trajectories is the controlled superposition of $\mathcal{F} = \Phi_B \circ \Phi_A$ and $\mathcal{G} = \Phi_A \circ \Phi_B$ where $\mathcal{F}$ and $\mathcal{G}$ are independent.

The coefficients α_0, α_1, β_0, and β_1 have also been referred to as vacuum amplitudes, with the resulting operations of $\alpha_0 B_j A_i$, $\alpha_1 A_k B_l$, $\beta_0 A_i$, and $\beta_1 B_j$ referred to as vacuum-extended channels, and any communication advantage of such channels is attributed to coherence with the vacuum
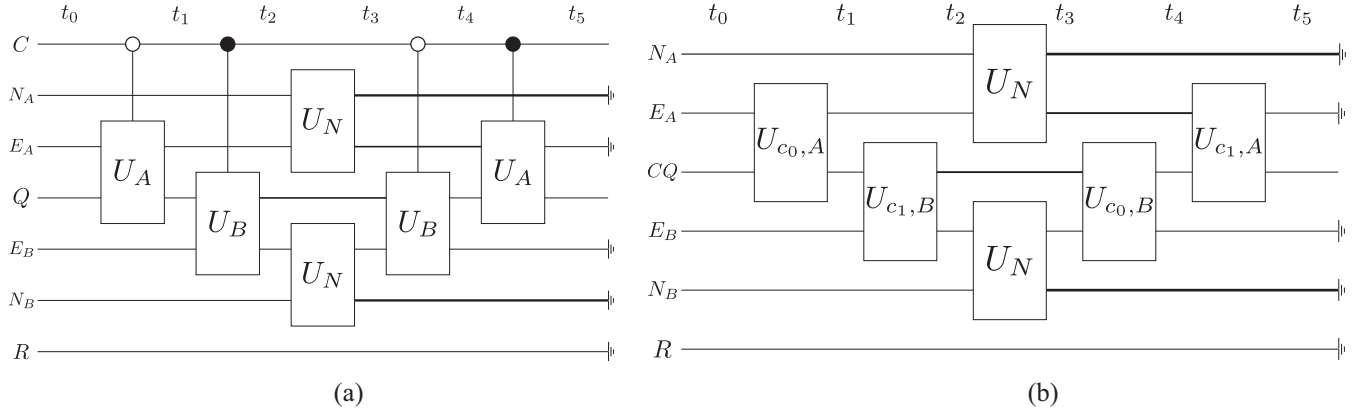
FIG. 5. (a) The environmental representation of a circuit that reduces to the two-party quantum switch if $U_N = I \otimes I$, where we have a superposition of orders. If $U_N = \text{SWAP}$, the circuit reduces to a superposition of trajectories where the environments E_A and E_B are not shared across time. (b) The same circuit as (a), but with systems C and Q grouped into a single party CQ. It should be noted that only systems C and Q or CQ are accessible to a receiver at the end of the circuit, for which a general decoding operation can be performed which is not shown in the diagram. Inaccessible systems are terminated with a ground symbol.

state which is absent in the quantum switch [34]. Furthermore, for a pair of entanglement-breaking channels with zero quantum capacity, the quantum switch allows the perfect activation of the quantum capacity, which is unachievable with the superposition of independent channels and trajectories [28].

Here in Fig. 5(a), not only is it clear that such a difference is due to the presence of non-Markovianity, where the $U_N = I \otimes I$ case of quantum switch can exhibit non-Markovianity, and the $U_N = \text{SWAP}$ case of superposition of trajectories is fully Markovian, the circuit also makes clear the presence of in-betweens where the amount of non-Markovianity can be controlled by the entangling capability of U_N. [Refer to the Appendix for proofs that the $U_N = I \otimes I$ and $U_N = \text{SWAP}$ cases of Fig. 5(a) indeed correspond to Eqs. (47) and (49).]

The inclusion of the control system C in the controlled unitaries implies that the operations on system Q are now tripartite operations acting on systems with dimensions $d_C \otimes d_{E_A} \otimes d_Q$ or $d_C \otimes d_Q \otimes d_{E_B}$:

$$U_{c_0,A} = |0\rangle\langle 0|^C \otimes U_A^{E_A Q} + |1\rangle\langle 1|^C \otimes I^{E_A Q}, \quad (52)$$

$$U_{c_1,A} = |0\rangle\langle 0|^C \otimes I^{E_A Q} + |1\rangle\langle 1|^C \otimes U_A^{E_A Q}, \quad (53)$$

$$U_{c_0,B} = |0\rangle\langle 0|^C \otimes U_B^{Q E_B} + |1\rangle\langle 1|^C \otimes I^{Q E_B}, \quad (54)$$

$$U_{c_1,B} = |0\rangle\langle 0|^C \otimes I^{Q E_B} + |1\rangle\langle 1|^C \otimes U_B^{Q E_B}. \quad (55)$$

Both systems C and Q are the accessible systems that a receiver can measure or decode to receive information from the sender. In fact, access to the control system C is necessary to achieve the communication advantage of the quantum switch [27]. Therefore, we can group the systems C and Q as a single party as shown in Fig. 5(b). The entanglement monotone that we are concerned with is now the entanglement of the bipartite split between R and CQ as a single party, $\mathsf{E}(\rho^{R|CQ})$. Each control unitary can then be rewritten as a bipartite unitary in the operator Schmidt form in Eq. (35), acting on systems with dimensions of $d_{E_A} \otimes d_C d_Q$ or $d_C d_Q \otimes d_{E_B}$.

We also note that by controlling the unitaries, not only is the symmetry of the Schmidt strength $K_{\text{sch}}(U^{E|Q})$ about $q = 0.5$ broken for $K_{\text{sch}}(U^{E|CQ})$, the maximum achievable $K_{\text{sch}}(U^{E|CQ})$ is also reduced. This is plotted for U_q of Eq. (38) in Fig. 6. An intuitive explanation for this reduction is that by controlling U_q with a control qubit such that U_q is only applied if say $\rho^C = |0\rangle$, then one might imagine that Q and E are only entangled in one path of the superposition and not the other, and thus the maximum possible entanglement between Q and E is reduced.
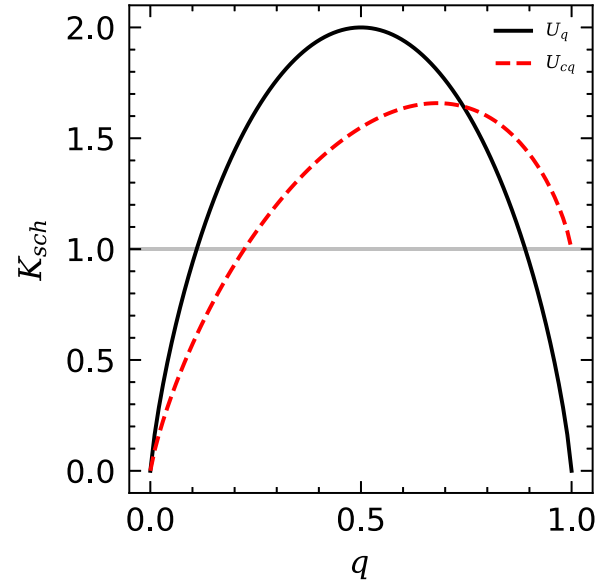

FIG. 6. Schmidt strength K_{sch} against the variable q of U_q in Eq. (38). The solid line shows $K_{\text{sch}}(U_q)$ where the Schmidt strength is symmetric and can reach a maximum of $K_{\text{sch}} = 2$ where it is maximally entangling. The dashed line shows $K_{\text{sch}}(U_{cq})$ where $U_{cq} = |0\rangle\langle 0| \otimes U_q + |1\rangle\langle 1| \otimes I$ due to the control of U_q with a control qubit. The symmetry about $q = 0.5$ is broken, and the maximum of $K_{\text{sch}} = 2$ cannot be reached.

Applying the monogamy relations, from $t_0 \to t_1$ and $t_1 \to t_2$, we have

$$E^\alpha\left(\rho_0^{R|N_A E_A E_B N_B(CQ)}\right) = E^\alpha\left(\rho_1^{R|N_A E_A E_B N_B(CQ)}\right),$$
$$\Delta_1 E^\alpha\left(\rho^{R|CQ}\right) = -E^\alpha\left(\rho_1^{R|E_A}\right) - E^\alpha\left(\rho_1^{R|\text{res}}\right), \quad (56)$$

$$E^\alpha\left(\rho_1^{R|N_A E_A E_B N_B(CQ)}\right) = E^\alpha\left(\rho_2^{R|N_A E_A E_B N_B(CQ)}\right),$$
$$\Delta_2 E^\alpha\left(\rho^{R|CQ}\right) = -E^\alpha\left(\rho_2^{R|E_B}\right) - \Delta_2 E^\alpha\left(\rho^{R|\text{res}}\right), \quad (57)$$

where again we applied Eqs. (24) and (25), and assumed that E_A, E_B, N_A, and N_B are initially pure and uncorrelated with CQ, R, and each other. Also note that since system CQ is taken

as a single party, we have

$$E^\alpha(\rho^{R|\text{res}}) = E^\alpha(\rho^{R|E_A N_A E_B N_B(CQ)}) - E^\alpha(\rho^{R|N_A})$$
$$- E^\alpha(\rho^{R|E_A}) - E^\alpha(\rho^{R|E_B})$$
$$- E^\alpha(\rho^{R|N_B}) - E^\alpha(\rho^{R|CQ}). \quad (58)$$

Here from Eq. (56) we see that our change of entanglement monotone in the first time step $\Delta_1 E^\alpha(\rho^{R|CQ}) \leqslant 0$ as expected. To show $\Delta_2 E^\alpha(\rho^{R|CQ}) \leqslant 0$, we note that the first two operations of $U_{c_0,A}$ and $U_{c_1,B}$ are simply the case in Fig. 1(c) with $U_N = \text{SWAP}$. Hence, the proof is the same as in Eq. (43) with the substitution of $E \to E_A$, $N \to E_B$, and $Q \to CQ$.

Next, for the operations of U_N, they each redistribute the bipartite entanglement of E_A and E_B to N_A, N_B, and multipartite entanglement. Hence, from $t_2 \to t_3$, we have

$$E^\alpha\left(\rho_2^{CQ|N_A E_A E_B N_B R}\right) = E^\alpha\left(\rho_3^{CQ|N_A E_A E_B N_B R}\right),$$
$$\Delta_3 E^\alpha(\rho^{CQ|E_A}) + \Delta_3 E^\alpha(\rho^{CQ|E_B}) = -E^\alpha\left(\rho_3^{CQ|N_A}\right) - E^\alpha\left(\rho_3^{CQ|N_B}\right) - \Delta_3 E^\alpha\left(\rho^{CQ|\text{res}}\right) \quad (59)$$

and

$$E^\alpha\left(\rho_2^{R|N_A E_A E_B N_B(CQ)}\right) = E^\alpha\left(\rho_3^{R|N_A E_A E_B N_B(CQ)}\right),$$
$$\Delta_3 E^\alpha(\rho^{R|E_A}) + \Delta_3 E^\alpha(\rho^{R|E_B}) = -E^\alpha\left(\rho_3^{R|N_A}\right) - E^\alpha\left(\rho_3^{R|N_B}\right) - \Delta_3 E^\alpha(\rho^{R|\text{res}}), \quad (60)$$

where we note that $E^\alpha(\rho_2^{R|CQ}) = E^\alpha(\rho_3^{R|CQ})$. Finally, for the last two operations from $t_3 \to t_4$ and $t_4 \to t_5$, we have

$$E^\alpha(\rho_3^{R|N_A E_A E_B N_B(CQ)}) = E^\alpha(\rho_4^{R|N_A E_A E_B N_B(CQ)}),$$
$$\Delta_4 E^\alpha\left(\rho^{R|CQ}\right) = -\Delta_4 E^\alpha\left(\rho^{R|E_B}\right) - \Delta_4 E^\alpha\left(\rho^{R|\text{res}}\right), \quad (61)$$

$$E^\alpha(\rho_4^{R|N_A E_A E_B N_B(CQ)}) = E^\alpha(\rho_5^{R|N_A E_A E_B N_B(CQ)}),$$
$$\Delta_5 E^\alpha\left(\rho^{R|CQ}\right) = -\Delta_5 E^\alpha\left(\rho^{R|E_A}\right) - \Delta_5 E^\alpha\left(\rho^{R|\text{res}}\right), \quad (62)$$

where again we see that any revival of the entanglement monotone with $\Delta_4 E^\alpha(\rho^{R|CQ}) \geqslant 0$ and $\Delta_5 E^\alpha(\rho^{R|CQ}) \geqslant 0$ must correspond to a decrease in the entanglement with the environments E_A or E_B, and a decrease in the multipartite residual entanglement. If we consider the Markovian case of $U_N = \text{SWAP}$, we have

$$E^\alpha\left(\rho_3^{R|E_B}\right) = E^\alpha\left(\rho_3^{R|E_A}\right) = E^\alpha\left(\rho_4^{R|E_A}\right) = 0, \quad (63)$$

and thus

$$E^\alpha\left(\rho_3^{R|E_B(CQ)}\right) = E^\alpha\left(\rho_4^{R|E_B(CQ)}\right),$$

$$\Delta_4 E^\alpha\left(\rho^{R|CQ}\right) = -E^\alpha\left(\rho_4^{R|E_B}\right) - \widetilde{E}^\alpha\left(\rho_4^{R|\text{res}}\right), \quad (64)$$

and

$$E^\alpha\left(\rho_4^{R|E_A(CQ)}\right) = E^\alpha\left(\rho_5^{R|E_A(CQ)}\right),$$
$$\Delta_5 E^\alpha\left(\rho^{R|CQ}\right) = -E^\alpha\left(\rho_5^{R|E_A}\right) - \bar{E}^\alpha\left(\rho_5^{R|\text{res}}\right), \quad (65)$$

where

$$\widetilde{E}^\alpha\left(\rho_4^{R|\text{res}}\right) = E^\alpha\left(\rho_4^{R|E_B(CQ)}\right) - E^\alpha\left(\rho_4^{R|CQ}\right) - E^\alpha\left(\rho_4^{R|E_B}\right),$$
$$\bar{E}^\alpha\left(\rho_5^{R|\text{res}}\right) = E^\alpha\left(\rho_5^{R|E_A(CQ)}\right) - E^\alpha\left(\rho_5^{R|E_A}\right) - E^\alpha\left(\rho_5^{R|CQ}\right). \quad (66)$$

Thus, we have $\Delta_4 E^\alpha(\rho^{R|CQ}) \leqslant 0$ and $\Delta_5 E^\alpha(\rho^{R|CQ}) \leqslant 0$ as expected for the fully Markovian system where our entanglement monotone decreases for all time steps.

It is also important to note that the operation $U_{c_0,B}$ from $t_3 \to t_4$ can affect the Markovianity of the operation $U_{c_1,A}$ in $t_4 \to t_5$. We can see this with

$$E^\alpha\left(\rho_3^{E_A|N_A E_B N_B R(CQ)}\right) = E^\alpha\left(\rho_4^{E_A|N_A E_B N_B R(CQ)}\right),$$
$$E^\alpha\left(\rho_3^{E_A|E_B}\right) + E^\alpha\left(\rho_3^{E_A|CQ}\right) + E^\alpha\left(\rho_3^{E_A|\text{res}}\right) = E^\alpha\left(\rho_4^{E_A|E_B}\right) + E^\alpha\left(\rho_4^{E_A|CQ}\right) + E^\alpha\left(\rho_4^{E_A|\text{res}}\right),$$
$$E^\alpha\left(\rho_4^{E_A|CQ}\right) = E^\alpha\left(\rho_3^{E_A|CQ}\right) - \Delta_4 E^\alpha(\rho^{E_A|E_B}) - \Delta_4 E^\alpha(\rho^{E_A|\text{res}}), \quad (67)$$

where we see that the operation of $U_{c_0,B}$ in $t_3 \to t_4$ can change the bipartite entanglement of $E_A|CQ$. If $E^\alpha(\rho_4^{E_A|CQ}) = 0$, then the operation of $U_{c_1,A}$ in $t_4 \to t_5$ must be Markovian, as E_A and

CQ are uncorrelated or, in other words, there is no memory in the environment as described in Sec. II B. This is only possible if $U_{c0,B}$ is maximally entangling, which cannot be achieved as

shown in Fig. 6. Thus, unlike the example in Fig. 1(c) where only U_2 is capable of revival of entanglement monotone, for the quantum switch, not only does the operation of both U_A and U_B allow revival, the amount of revival is also dependent on each other.

Ultimately, along with its CP indivisibility, the non-monotonicity and possibility of revival for the entanglement monotone of the bipartite entanglement of $R|CQ$ from $t_3 \to t_4$ and $t_4 \to t_5$, imply that this implementation of the two-party quantum switch has intrinsic non-Markovianity in its operation in those time steps. The system will be Markovian with no possibility of information revival if we stop the operation of the circuit at time step t_2, which results in the case in Ref. [31] of a controlled superposition of two independent channels as in Eq. (51), and its enhancements might be attributed to the reduction of entangling capacity due to the addition of the control as shown in Fig. 6.

Non-Markovianity only comes in with the inclusion of the last two operations from $t_3 \to t_5$ which completes the two-party quantum switch. Again, be reminded that CP indivisibility does not imply information or entanglement monotone revival, and thus the last two operations can either reduce or enhance, via information revival, communication capacity of the entire circuit, which conforms with the results in Ref. [25] where the Holevo quantities of arbitrary channels were computed for the quantum switch, and shown to either performs better or worse than the superposition of two independent channels. Such a comparison corresponds to comparing the Holevo quantity at t_5 and t_2 of the circuit in Fig. 5(a), with $U_N = I \otimes I$.

Here, we show this numerically and show that this variability in performance when compared to the superposition of independent channels depends on the entangling capabilities of the operations involved. We note that without loss of generality, the system has dimensions of $d_R \otimes d_{N_A} \otimes d_{N_B} d_{E_A} d_{E_B} d_{CQ} = 2 \otimes 2 \otimes 2^5$, for which the monogamy relation still holds for concurrence squared [69]. Note, however, that concurrence for mixed states that are not $d_A \otimes d_B = 2 \otimes 2$ is defined via its associated EoF or convex roof extension as in Eq. (22). Furthermore, since we have $C^2(|\psi\rangle) = 2S_2(|\psi\rangle)$, where

$$S_2(|\psi\rangle^{AB}) = 1 - \text{Tr}[(\rho^A)^2] \qquad (68)$$

is the linear entropy with $\rho^A = \text{Tr}_B(|\psi\rangle\langle\psi|^{AB})$, we can define the convex roof extension of concurrence squared as

$$\frac{1}{2}C^2(\rho^{A|B}) = S_2(\rho^{A|B}) = \min_{\{p_i, |\psi_i\rangle\}} \sum_i p_i S_2(|\psi_i\rangle), \qquad (69)$$

where the minimization is taken over all pure state decompositions $\rho^{AB} = \sum_i p_i |\psi_i\rangle\langle\psi_i|$.

As party CQ has dimensions of $d_C d_Q = 4$ for qubits, we require the computation of concurrence squared for mixed states of $d_R \otimes d_C d_Q = 2 \otimes 4$ dimensional system for $C^2(\rho^{R|CQ})$. While such a minimization is nontrivial in general, the linear entropy can be expressed in the form of an expectation value, and thus its convex roof extension in Eq. (69) can be expressed

as a semidefinite program (SDP) of

$$\text{minimize} \quad S_2(\rho) = \text{Tr}[\mathcal{A}_{AA'}\omega_{12}],$$

$$\text{s.t.} \quad \omega_{12} = \omega_{12}^\dagger, \ \omega_{12}^{T_1} \geqslant 0,$$

$$\text{Tr}_1(\omega_{12}) = \text{Tr}_2(\omega_{12}) = \rho, \qquad (70)$$

where

$$\omega_{12} = \sum_i p_i |\psi_i\rangle\langle\psi_i| \otimes |\psi_i\rangle\langle\psi_i|, \qquad (71)$$

and $\mathcal{A}_{AA'} = I_{AA'BB'} - (\text{SWAP}_{AA'} \otimes I_{BB'})$ is a projector to the antisymmetric space of AB and its second copy $A'B'$ [76]. The SDP is a convex optimization problem that can be solved efficiently with several algorithms, and thus allows the computation of the concurrence squared of bipartite mixed states of arbitrary dimensions [77].

Taking U_A, U_B, and U_N as U_q in Eq. (38), an input system Q of Eq. (46) with $p = 0.5$, and $\rho_0^C = |+\rangle\langle+|$, the change in concurrence squared $\Delta C^2(\rho^{R|CQ})$ is plotted as a color map in a contour plot against variables q_A, q_B, and n of U_q for U_A, U_B, and U_N. Figures 7(a) and 7(b) show the plot for $t_3 \to t_4$ and $t_4 \to t_5$ respectively.

Similar to the single-pass case of Fig. 1(c), the maximum amount of revival decreases for increasing entangling capability of U_N, until the maximally entangling case of $n = 0.5$ with $K_{\text{sch}}(U_N) = 2$ where no revival is observed for all values of q_A and q_B. The ranges of q_A and q_B that do not grant a revival are eternally non-Markovian processes where its non-Markovianity is "hidden" [46,47], which explains the inconsistency in the quantum switch's enhancement in Ref. [25]. We emphasize that in Fig. 5, the best choice of U_N for the revival of the entanglement monotone is the quantum switch case of $U_N = I \otimes I$ with $n = 0$ where we have full non-Markovianity. As such, any choices of q_A and q_B that can result in revival for the general case of $U_N \neq I \otimes I$, should also result in revival for the quantum switch case of $U_N = I \otimes I$ since any nonlocal U_N will reduce the the amount of non-Markovianity as discussed in Sec. II B.

We visualize this in Fig. 8 for $n = 0$, 0.015, and 0.03 in the time steps of $t_3 \to t_5$ where non-Markovian revival is possible. Not only do we see the areas of q_A and q_B where revivals are possible decrease with increasing n, their revival magnitudes are also decreasing. More importantly, these areas where revivals are possible for larger values of n are contained within the smaller values of n. In other words, any choices of q_A and q_B that can result in a revival for a specific n will result in an even greater revival for a $n' < n$.

B. Example: Entanglement-breaking channels

An entanglement-breaking channel Φ_* acting on an information-carrying system Q with $(\Phi_* \otimes I)|QR\rangle$ completely destroys the bipartite entanglement between $Q|R$, i.e., zero entanglement monotone, leading to zero coherent information, and thus zero quantum capacity [78]. Such channels have a measure-and-reprepare form of

$$\Phi_*(\rho^Q) = \sum_k |\psi_k\rangle\langle\psi_k|\langle\phi_k|\rho^Q|\phi_k\rangle, \qquad (72)$$

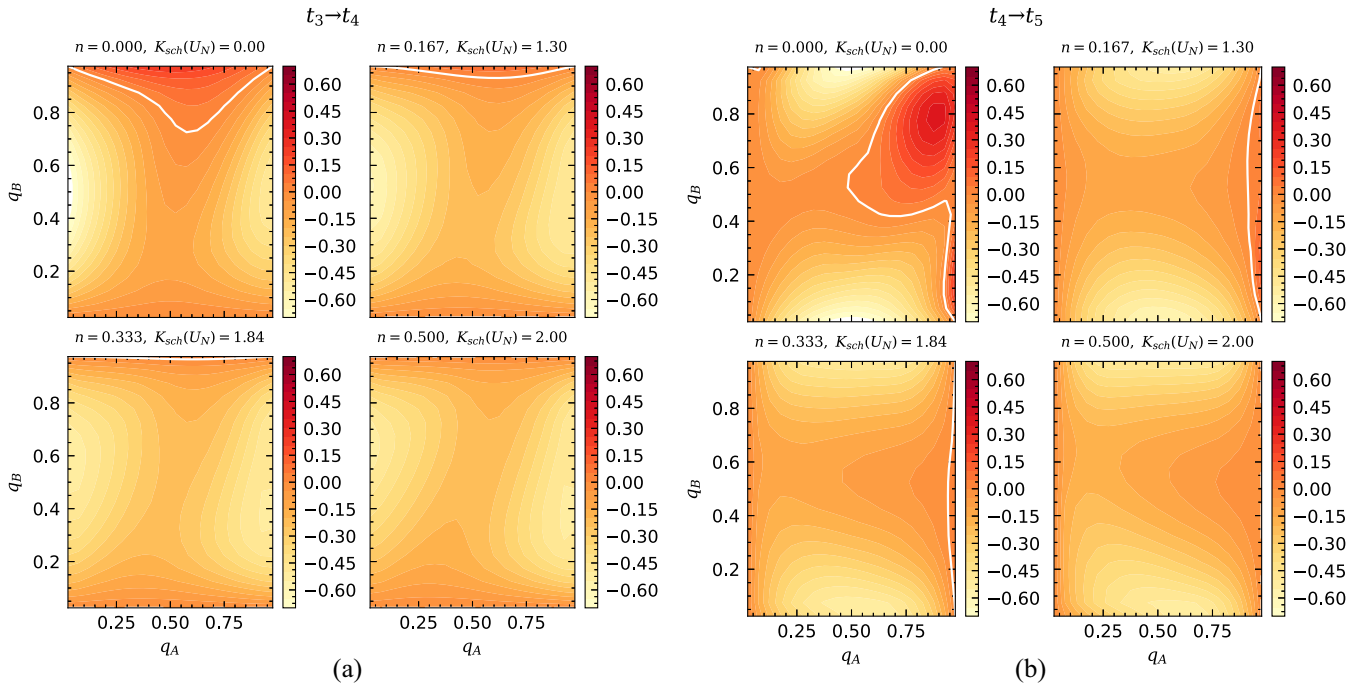where $\sum_k |\phi_k\rangle\langle\phi_k| = I$.

FIG. 7. The change in the entanglement monotone of concurrence squared $\Delta C^2(\rho^{R|CQ})$ of $R|CQ$ (shown as the color map) from (a) $t_3 \rightarrow t_4$ and (b) $t_4 \rightarrow t_5$ for $p = 0.5$. The white lines are values of q_A and q_B that have zero change in concurrence squared, and are the boundaries between positive and negative changes. The amount of revival is largest for $n \rightarrow 0$, and disappears for $n \rightarrow 0.5$, as the system approaches to a Markovian process. Revival is observed for both the operation of $U_{c_0,B}$ from $t_3 \rightarrow t_4$ and of $U_{c_1,A}$ from $t_4 \rightarrow t_5$.

In Ref. [28], it was shown that if two entanglement-breaking channels are placed in the quantum switch setup, it enables perfect quantum communication, i.e., the initial and final coherent information are equal. On the other hand, this perfect activation of quantum capacity was not achievable if the channels are placed in a superposition of independent channels or trajectories, albeit some activation is still possible. Such a difference in advantage was attributed to the difference between a superposition of independent paths or trajectories, and a superposition of alternate causal orders. Here, we repli-

cate this result numerically in our framework and suggest that this perfect activation is indicative of the presence of non-Markovianity.

First, referring to Fig. 5(a), recall that if we were to stop the operation of the quantum switch at t_2, we obtain the circuit for the superposition of two independent channels as in Eq. (51). Therefore, the comparison between the quantum switch and a superposition of two independent channels discussed in Ref. [28] is in fact a comparison between the quantum capacities at t_5 and t_2. As the process from t_2 to t_5 is
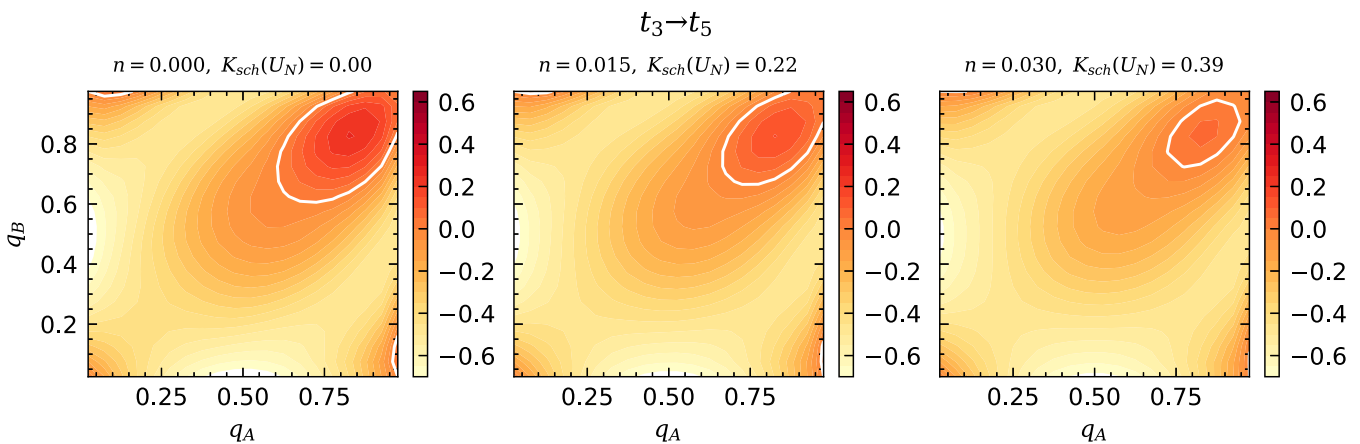

FIG. 8. The change in the entanglement monotone of concurrence squared $\Delta C^2(\rho^{R|CQ})$ of $R|CQ$ (shown as the color map) for the total non-Markovian revival time steps of $t_3 \rightarrow t_5$ for $p = 0.5$. The white lines are values of q_A and q_B that have zero change in concurrence squared, and are the boundaries between positive and negative changes. The area and amount of revival is largest for the quantum switch case of $n = 0$, and decreases for increasing n as the amount of non-Markovianity in the system reduces. The bounded areas of the larger values of n are within the bounded areas of the smaller values.
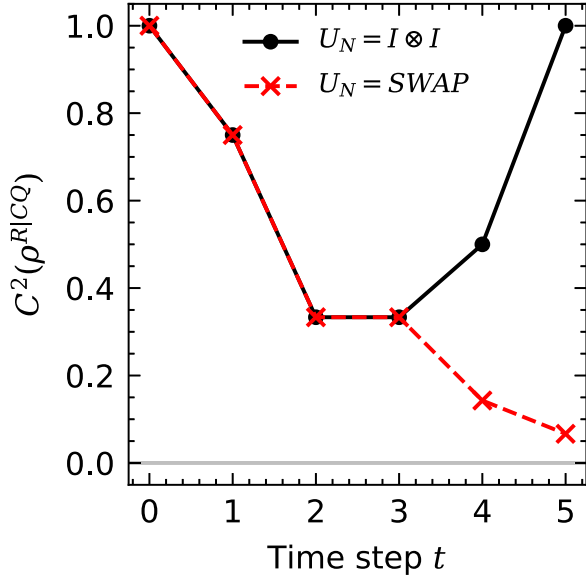
FIG. 9. Entanglement monotone of concurrence squared $C^2(\rho^{R|CQ})$ of bipartite split $R|CQ$ at each time step for the circuit in Fig. 5(a) with entanglement-breaking channels. For the quantum switch case of $U_N = I \otimes I$, perfect revival is observed from $t_3 \rightarrow t_5$, granting perfect activation for the coherent information. For the Markovian case of $U_N = \text{SWAP}$, there is no revival as expected as C^2 is monotonic.

non-Markovian in general, any possible advantage the quantum switch has over the superposition of independent channels can be thought of as a revival or backflow of information due to its non-Markovianity. Similarly, the comparison with a superposition of trajectories as in Eq. (49) corresponds to a comparison between the quantum switch case of $U_N = I \otimes I$, and the Markovian case of $U_N = \text{SWAP}$.

The entanglement-breaking channel discussed in Ref. [28] has Kraus operators of

$$\{K_i\} = \left\{ \frac{X}{\sqrt{2}}, \frac{Y}{\sqrt{2}} \right\}. \tag{73}$$

In the environmental representation of Fig. 5(a), we have

$$U_A = U^{E_A Q} = \begin{pmatrix} [K_1] & [K_2] \\ [K_2] & [K_1] \end{pmatrix} \tag{74}$$

$$= \frac{1}{\sqrt{2}} \begin{pmatrix} X & Y \\ Y & X \end{pmatrix}, \tag{75}$$

where X and Y are block matrices, and similarly

$$U_B = U^{Q E_B} = \text{SWAP}\, U^{E_A Q}\, \text{SWAP}. \tag{76}$$

The entanglement monotone of concurrence squared of $R|CQ$ for each time step is then computed via the SDP in Eq. (70) and plotted in Fig. 9 for the quantum switch with $U_N = I \otimes I$ and the Markovian case with $U_N = \text{SWAP}$. Again, from $t_0 \rightarrow t_2$ we have the superposition of two independent channels, for which some activation of coherent information is possible as the entanglement monotone $C^2(\rho^{R|CQ})$ is nonzero. As discussed previously, such activation might be due to the reduction of entangling capability by the coherent control of

superposition as shown in Fig. 6. On the other hand, for the quantum switch with $U_N = I \otimes I$, we have a perfect revival of the entanglement monotone, and thus coherent information, from $t_3 \rightarrow t_5$. This revival is absent for the Markovian case of $U_N = \text{SWAP}$ which results in the superposition of trajectories, but similar to the superposition of two independent channels, some activation is still possible as the final entanglement monotone is nonzero.

Therefore, we replicated numerically the perfect activation of coherent information in Ref. [28], and note that such an activation is only possible with the presence of non-Markovianity. Additionally, we note again that when given a pair of noisy quantum channels, the quantum switch setup will outperform a superposition of the two independent channels, where we stop the operation at t_2, if there is a net positive revival of information from $t_3 \rightarrow t_5$ due to non-Markovianity.

C. Non-Markovianity without indefinite causal order

The presence of non-Markovianity depends on the presence of memory in the environment or, in other words, whether the environment is shared between different operations over time. Therefore, for the quantum switch circuit in Fig. 5(a), non-Markovianity is still present even if the operations from time steps $t_3 \rightarrow t_4$ and $t_4 \rightarrow t_5$ are not U_B and U_A, provided $U_N \neq \text{SWAP}$.

We label the unitaries at different time steps in Fig. 5(a) as $U_{t_0 \rightarrow t_1}$, $U_{t_1 \rightarrow t_2}$, $U_{t_3 \rightarrow t_4}$, and $U_{t_4 \rightarrow t_5}$, respectively. Note that we set the fully non-Markovian case of $U_N = I \otimes I$ which is omitted in this discussion. We obtain the quantum switch with indefinite causal order if $U_{t_3 \rightarrow t_4} = U_{t_1 \rightarrow t_2}$, and $U_{t_4 \rightarrow t_5} = U_{t_0 \rightarrow t_1}$ as shown in Fig. 5(a) with $U_{t_0 \rightarrow t_1} = U_{t_4 \rightarrow t_5} = U_A$ and $U_{t_1 \rightarrow t_2} = U_{t_3 \rightarrow t_4} = U_B$.

Here, we demonstrate numerically that the communication enhancement with $U_{t_3 \rightarrow t_4} \neq U_{t_1 \rightarrow t_2}$ and $U_{t_4 \rightarrow t_5} \neq U_{t_0 \rightarrow t_1}$, i.e., no indefinite causal order, can also be achieved. We generate random pairs of unitaries for $U_{t_0 \rightarrow t_1}$ and $U_{t_1 \rightarrow t_2}$, and compare the quantum switch case of $U_{t_3 \rightarrow t_4} = U_{t_1 \rightarrow t_2}$ and $U_{t_4 \rightarrow t_5} = U_{t_0 \rightarrow t_1}$ with the more general case of $U_{t_3 \rightarrow t_4} \neq U_{t_1 \rightarrow t_2}$ and $U_{t_4 \rightarrow t_5} \neq U_{t_0 \rightarrow t_1}$, where $U_{t_4 \rightarrow t_5}$ and $U_{t_3 \rightarrow t_4}$ are also pairs of randomly generated unitaries. The effective channel of the more general case has Kraus operators of

$$K_{ij}^{\text{gen}} = |0\rangle\langle 0| \otimes C_j A_i + |1\rangle\langle 1| \otimes D_i B_j, \tag{77}$$

where the sets of Kraus operators $\{A_i\}$, $\{B_i\}$, $\{C_i\}$, and $\{D_i\}$ are the Kraus operators for the channels Φ_A, Φ_B, Φ_C, and Φ_D, which corresponds to the unitary operations of $U_{t_0 \rightarrow t_1}$, $U_{t_1 \rightarrow t_2}$, $U_{t_4 \rightarrow t_5}$, and $U_{t_3 \rightarrow t_4}$, respectively [the proof follows from the proof of Eq. (47) in the Appendix simply by relabeling the unitaries]. Note that the presence of non-Markovianity implies that the effective operations of Φ_C and Φ_D from $t_3 \rightarrow t_5$ are not CPTP operations. We denote σ as the output state of the general case with $\sigma^{CQ} = \sum_{ij} K_{ij}^{\text{gen}}(\rho^C \otimes \rho^Q) K_{ij}^{\text{gen}\dagger}$, in contrast to ρ^{CQ} used for the quantum switch. We illustrate this difference between the quantum switch and the general case in the space-time diagrams of the channel operations in Fig. 10, where Fig. 10(a) shows the space-time diagram of the operation of a quantum switch with the channels Φ_A and Φ_B placed in a superposition of alternate orders, and in Fig. 10(b) we have the general case where the final two operations are
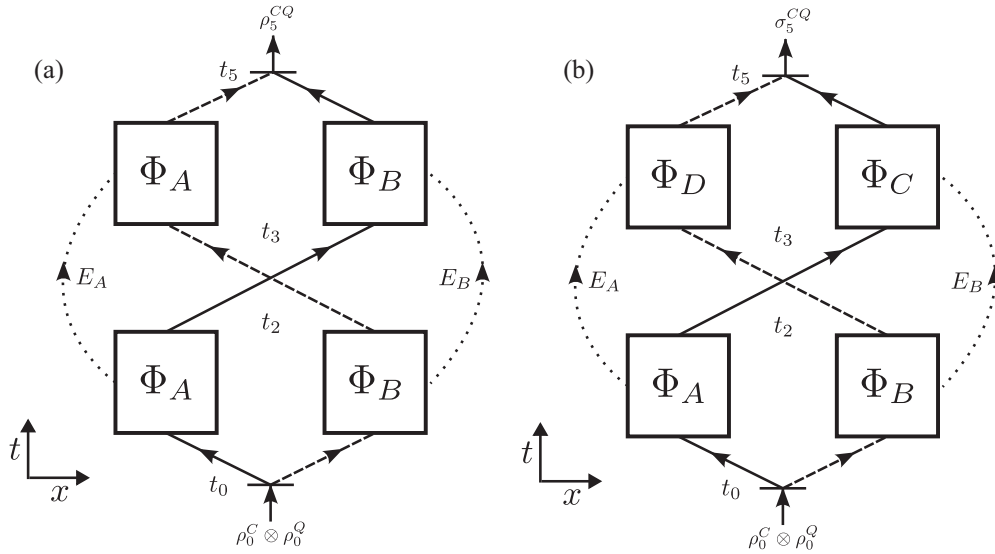
FIG. 10. (a) The space-time diagram of a quantum switch where the channels Φ_A and Φ_B are placed in a controlled superposition of alternate causal orders. (b) The space-time diagram of the general case circuit where the last two operations are replaced with different channels of Φ_C and Φ_D. The solid and dashed lines indicate the two different paths of the controlled superposition, and the dotted lines indicate the sharing of the environments or non-Markovian memories between the channel operations. Also note that time steps $t_0 \rightarrow t_1$ and $t_1 \rightarrow t_2$ are combined into a single time step $t_0 \rightarrow t_2$ in the diagram, and vice versa for time steps $t_3 \rightarrow t_4$ and $t_4 \rightarrow t_5$ with the time step $t_3 \rightarrow t_5$.

replaced with channels Φ_C and Φ_D. It is important to note that similar to the quantum switch, the environments or non-Markovian memories in E_A and E_B are still shared between the operations in the general case.

The concurrence squared, Holevo quantity, and coherent information of the general case output $\sigma_5^{R|CQ}$ is plotted against that of the quantum switch output $\rho_5^{R|CQ}$ in Fig. 11. The vertical lines are the ranges of values obtained by the random search of unitaries $U_{t_3 \rightarrow t_4}$ and $U_{t_4 \rightarrow t_5}$ for a fixed pair of $U_{t_0 \rightarrow t_1}$ and $U_{t_1 \rightarrow t_2}$, while the scatter points are their respective means. The presence of points or ranges above the diagonal dashed line implies that there are choices of $U_{t_3 \rightarrow t_4} \neq U_{t_1 \rightarrow t_2}$ and $U_{t_4 \rightarrow t_5} \neq U_{t_0 \rightarrow t_1}$ that can grant communication advantages

similar to the quantum switch, all without the presence of indefinite causal order.

Such a comparison is different from Refs. [31] and [28] where the quantum switch was compared to a superposition of two independent channels, which has different circuit structures, and that the information-carrying system was operated on by a fewer number of channels [34], here the comparison is made with a set of composed channels that are different.

In this more general construction, we simply ask what are the best choices of channels Φ_C and Φ_D that can lead to a large amount of information revival, and showed that there are choices that are better than the quantum switch's choice of $\Phi_C = \Phi_B$ and $\Phi_D = \Phi_A$. One might also think that any
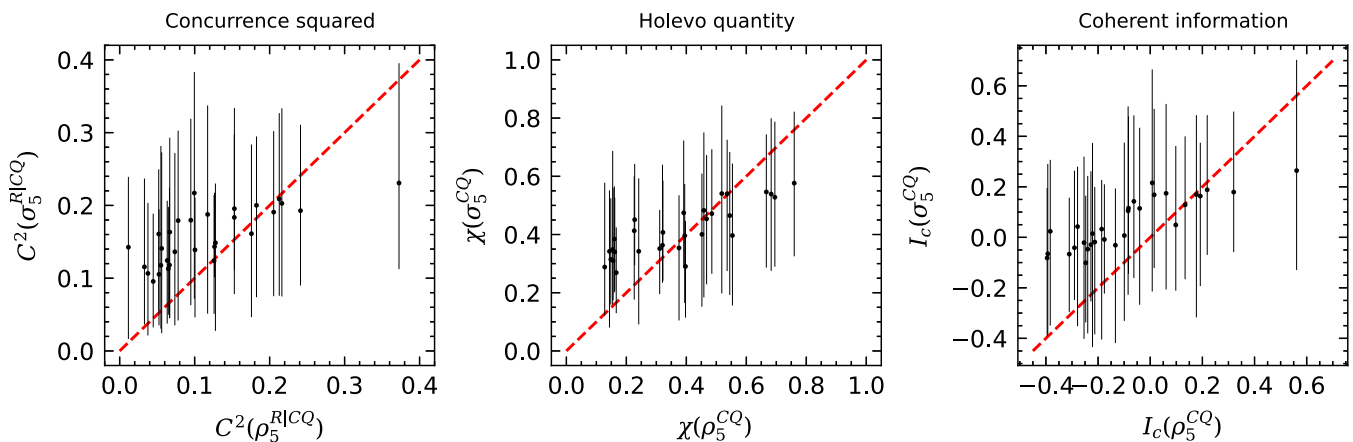

FIG. 11. The concurrence squared, Holevo quantity, and coherent information of the general case of $U_{t_3 \rightarrow t_4} \neq U_{t_1 \rightarrow t_2}$ and $U_{t_4 \rightarrow t_5} \neq U_{t_0 \rightarrow t_1}$ plotted against the quantum switch case of $U_{t_3 \rightarrow t_4} = U_{t_1 \rightarrow t_2}$ and $U_{t_4 \rightarrow t_5} = U_{t_0 \rightarrow t_1}$. The vertical lines are the ranges of values of the randomly searched $U_{t_3 \rightarrow t_4}$ and $U_{t_4 \rightarrow t_5}$ for a fixed pair of $U_{t_0 \rightarrow t_1}$ and $U_{t_1 \rightarrow t_2}$, and the scatter points are their means. Points or ranges above the diagonal dashed line are unitaries where the general case performs better than the quantum switch.

advantages of the general case can be trivially achieved if channels Φ_C and Φ_D are less noisy than channels Φ_A and Φ_B. However, this is not true as if the channels Φ_C and Φ_D are the least noisy case of identity channels, then no revival of information is possible, and the circuit might perform worse than the quantum switch. Furthermore, we note that Eq. (77) does not depend on their local vacuum extensions described in the "mode picture" of Ref. [33].

For the quantum switch, two closed laboratories will perform Φ_A and Φ_B each with no knowledge of the outside global causal structure, and the orders for which a signal is sent to the two laboratories are then placed in a controlled superposition. On the other hand, the general case might require each laboratory to perform different operations at different time steps while maintaining the memory in the environment. How this general case might be implemented and whether it is a physically possible task is outside the scope of this paper.

V. CONCLUSION

We introduced a framework in the environmental representation that accounts for non-Markovianity for the quantum compositions of channels, and deduced that the two-party quantum switch is intrinsically a non-Markovian process by implementing it in this framework. In our approach, the flow of entanglement in the information-carrying system can be quantified using the monogamy relation, and the revival of the entanglement monotone suggests that this implementation of the quantum switch's communication advantages are not impartial to this non-Markovianity.

Comparisons of the communication capacities of the quantum switch and a superposition of two independent channels made in various studies of the quantum switch [25,31,33,34] were also made clear in this framework as a comparison between two time steps t_2 and t_5 in Figs. 5(a) and 10(a), such that any advantages the quantum switch has over the superposition of independent channels are only manifest with non-Markovian revival of information from time steps $t_3 \rightarrow t_5$. The presence of eternally non-Markovian processes where non-Markovianity does not lead to revival from time steps $t_3 \rightarrow t_5$ also explains the inconsistency of the quantum switch's enhancement when compared to the superposition of independent channels at t_2 in Ref. [25], and of course for a fully Markovian system of $U_N = \text{SWAP}$ where the system reduces to a superposition of trajectories, no revival is possible.

The perfect activation of coherent information with entanglement-breaking channels [28] was also captured by this framework as a revival in $t_3 \rightarrow t_5$, and we expect this to be true for other cases of causal activation or enhance-

ment as long as the measure in question is an information monotone, such as in Ref. [27] where the causal activation of Holevo information was shown for a pair of completely depolarizing channels. This non-Markovian revival of information from time steps $t_3 \rightarrow t_5$ is crucial in buffering up the communication capacities of the system, and it was shown that communication enhancements are possible as long as this non-Markovianity is present, even without the presence of indefinite causal orders.

However, it is important to note that this construction of the quantum switch relies on correlations in time or the presence of memory in the environment, which is the basis of its non-Markovianity. Therefore, such a setup does not include implementations of indefinite causal order that can be achieved by means that are not captured in this framework, such as those caused by a superposition of space-times or gravitational time dilation [79–82]. However, our implementation mimics current experimental implementations of the quantum switch which are multipath photonics setup [35–38]. Whether these implementations are a genuine implementation of indefinite causal orders [39] are outside the scope of this paper. Nevertheless, the various communication enhancements of the quantum switch relies on the Kraus representation in Eq. (47), which is also the effective channel for our non-Markovian implementation of the quantum switch. Hence, we hope that our framework can offer insights to the workings of the phenomenon of causal activation, even if it might not be a physical interpretation of it.

While we have demonstrated that the presence and absence of revival of entanglement monotone, and thus enhancement and reduction in communication capacities, are dependent on the entangling capabilities of the bipartite unitaries, the exact quantitative relation is still unclear and varies with different circuit structures. A natural future work is to uncover these relations and determine the conditions for revival of information. We have also taken a nonoperational approach with the environmental representation; other future works on the non-Markovianity of the quantum switch can take an operational approach, and a resource theory of non-Markovianity can be applied to the quantum switch. Furthermore, it is unclear whether non-Markovianity also plays a role in other advantages of the quantum switch such as its computational advantages [15–17] or in work extractions [21,22]. Moving away from the quantum switch, the search for an ideal communication structure to maximize revival or backflow of information given a set of channels is also significant for efficient transmission of information in a quantum network with multiple communication parties, and ultimately a step towards the goal of a quantum internet.

APPENDIX: PROOF OF ENVIRONMENTAL REPRESENTATION OF QUANTUM SWITCH

Here, we will show that the environmental representation in Fig. 5(a) with $U_N = I \otimes I$ reduces to the quantum switch operation with Kraus operators of Eq. (47), and that with $U_N = \text{SWAP}$ it reduces to the superposition of trajectories operation with Kraus operators of Eq. (49).

We set the initial states as $\rho^C \otimes \rho^{E_A} \otimes \rho^Q \otimes \rho^{E_B}$, noting that $\rho^{E_A} = |e_A\rangle\langle e_A|$ and $\rho^{E_B} = |e_B\rangle\langle e_B|$ are pure. We can omit systems N_A and N_B as they do not interact with the rest of the system with $U_N = I \otimes I$. Therefore, the circuit's operation for

$U_N = I \otimes I$ is

$$
\begin{aligned}
\operatorname{Tr}_{E_A,E_B}\big[\big(&|0\rangle\langle 0|^C \otimes I^{E_A} \otimes I^Q \otimes I^{E_B} + |1\rangle\langle 1|^C \otimes U_A^{E_A Q} \otimes I^{E_B}\big)\big(|0\rangle\langle 0|^C \otimes I^{E_A} \otimes U_B^{QE_B} + |1\rangle\langle 1|^C \otimes I^{E_A} \otimes I^Q \otimes I^{E_B}\big) \\
&\times \big(|0\rangle\langle 0|^C \otimes I^{E_A} \otimes I^Q \otimes I^{E_B} + |1\rangle\langle 1|^C \otimes I^{E_A} \otimes U_B^{QE_B}\big)\big(|0\rangle\langle 0|^C \otimes U_A^{E_A Q} \otimes I^{E_B} + |1\rangle\langle 1|^C \otimes I^{E_A} \otimes I^Q \otimes I^{E_B}\big) \\
&\times \big(\rho^C \otimes \rho^{E_A} \otimes \rho^Q \otimes \rho^{E_B}\big) \\
&\times \big(|0\rangle\langle 0|^C \otimes U_A^{E_A Q} \otimes I^{E_B} + |1\rangle\langle 1|^C \otimes I^{E_A} \otimes I^Q \otimes I^{E_B}\big)^\dagger \big(|0\rangle\langle 0|^C \otimes I^{E_A} \otimes I^Q \otimes I^{E_B} + |1\rangle\langle 1|^C \otimes I^{E_A} \otimes U_B^{QE_B}\big)^\dagger \\
&\times \big(|0\rangle\langle 0|^C \otimes I^{E_A} \otimes U_B^{QE_B} + |1\rangle\langle 1|^C \otimes I^{E_A} \otimes I^Q \otimes I^{E_B}\big)^\dagger \big(|0\rangle\langle 0|^C \otimes I^{E_A} \otimes I^Q \otimes I^{E_B} + |1\rangle\langle 1|^C \otimes U_A^{E_A Q} \otimes I^{E_B}\big)^\dagger\big] \\
= \operatorname{Tr}_{E_A,E_B}\big[\big(&|0\rangle\langle 0|^C \otimes \big(I^{E_A} \otimes U_B^{QE_B}\big)\big(U_A^{E_A Q} \otimes I^{E_B}\big) + |1\rangle\langle 1|^C \otimes \big(U_A^{E_A Q} \otimes I^{E_B}\big)\big(I^{E_A} \otimes U_B^{QE_B}\big)\big) \\
&\times \big(\rho^C \otimes |e_A\rangle\langle e_A| \otimes \rho^Q \otimes |e_B\rangle\langle e_B|\big) \\
&\times \big(|0\rangle\langle 0|^C \otimes \big(I^{E_A} \otimes U_B^{QE_B}\big)\big(U_A^{E_A Q} \otimes I^{E_B}\big) + |1\rangle\langle 1|^C \otimes \big(U_A^{E_A Q} \otimes I^{E_B}\big)\big(I^{E_A} \otimes U_B^{QE_B}\big)\big)^\dagger\big]
\end{aligned}
$$

$$
\begin{aligned}
= \sum_{i,j}^{d^2} \bigg(&|0\rangle\langle 0|^C \otimes \overbrace{(I \otimes \langle j|)U_B^{QE_B}(I \otimes |e_B\rangle)}^{B_j}\,\overbrace{(\langle i| \otimes I)U_A^{E_A Q}(|e_A\rangle \otimes I)}^{A_i} \\
&+ |1\rangle\langle 1|^C \otimes \overbrace{(\langle i| \otimes I)U_A^{E_A Q}(|e_A\rangle \otimes I)}^{A_i}\,\overbrace{(I \otimes \langle j|)U_B^{QE_B}(I \otimes |e_B\rangle)}^{B_j}\,g)(\rho^C \otimes \rho^Q) \\
&\times \bigg(|0\rangle\langle 0|^C \otimes \overbrace{(\langle e_A| \otimes I)U_A^{E_A Q\dagger}(|i\rangle \otimes I)}^{A_i^\dagger}\,\overbrace{(I \otimes \langle e_B|)U_B^{QE_B\dagger}(I \otimes |j\rangle)}^{B_j^\dagger} \\
&+ |1\rangle\langle 1|^C \otimes \overbrace{(I \otimes \langle e_B|)U_B^{QE_B\dagger}(I \otimes |j\rangle)}^{B_j^\dagger}\,\overbrace{(\langle e_A| \otimes I)U_A^{E_A Q\dagger}(|i\rangle \otimes I)}^{A_i^\dagger}\bigg)
\end{aligned}
$$

$$
= \sum_{i,j}^{d^2} (|0\rangle\langle 0|^C \otimes B_j A_i + |1\rangle\langle 1|^C \otimes A_i B_j)(\rho^C \otimes \rho^Q)(|0\rangle\langle 0|^C \otimes A_i^\dagger B_j^\dagger + |1\rangle\langle 1|^C \otimes B_j^\dagger A_i^\dagger)
$$

$$
= \sum_{i,j}^{d^2} K_{ij}^{\text{sw}}(\rho^C \otimes \rho^Q)K_{ij}^{\text{sw}\dagger}, \tag{A1}
$$

where we obtained the quantum switch operations with Kraus operators of Eq. (47).

Similarly, for the case of $U_N = \text{SWAP}$ where $\rho^{N_A} = |n_A\rangle\langle n_A|$ and $\rho^{N_B} = |n_B\rangle\langle n_B|$ are pure states, the circuit operation results in an operation with Kraus operators of Eq. (49):

$$
\begin{aligned}
\operatorname{Tr}_{E_A,E_B,N_A,N_B}\big[\big(&|0\rangle\langle 0|^C \otimes \big(I^{N_A} \otimes I^{E_A} \otimes U_B^{QN_B} \otimes I^{B_1}\big)\text{SWAP}^{E_B N_B}\big(I^{N_A} \otimes U_A^{E_A Q} \otimes I^{E_B} \otimes I^{N_B}\big) \\
&+ |1\rangle\langle 1|^C \otimes \big(I^{E_A} \otimes U_A^{N_A Q} \otimes I^{E_B} \otimes I^{B_2}\big)\text{SWAP}^{N_A E_A}\big(I^{N_A} \otimes I^{E_A} \otimes U_B^{QE_B} \otimes I^{N_B}\big)\big) \\
&\times \big(\rho^C \otimes |n_A\rangle\langle n_A| \otimes |e_A\rangle\langle e_A| \otimes \rho^Q \otimes |e_B\rangle\langle e_B| \otimes |n_B\rangle\langle n_B|\big) \\
&\times \big(|0\rangle\langle 0|^C \otimes \big(I^{N_A} \otimes I^{E_A} \otimes U_B^{QN_B} \otimes I^{B_1}\big)\text{SWAP}^{E_B N_B}\big(I^{N_A} \otimes U_A^{E_A Q} \otimes I^{E_B} \otimes I^{N_B}\big) \\
&+ |1\rangle\langle 1|^C \otimes \big(I^{E_A} \otimes U_A^{N_A Q} \otimes I^{E_B} \otimes I^{B_2}\big)\text{SWAP}^{N_A E_A}\big(I^{N_A} \otimes I^{E_A} \otimes U_B^{QE_B} \otimes I^{N_B}\big)\big)^\dagger\big]
\end{aligned}
$$

$$
\begin{aligned}
= \sum_{i,j,k,l}^{d^2} \bigg(&|0\rangle\langle 0|^C \otimes \langle k|n_A\rangle \otimes \overbrace{(I \otimes \langle j|)U_B^{QN_B}(I \otimes |n_B\rangle)}^{B_j}\,\overbrace{(\langle i| \otimes I)U_A^{E_A Q}(|e_A\rangle \otimes I)}^{A_i} \otimes \langle l|e_B\rangle \\
&+ |1\rangle\langle 1|^C \otimes \langle i|e_A\rangle \otimes \overbrace{(\langle k| \otimes I)U_A^{N_A Q}(|n_A\rangle \otimes I)}^{A_k}\,\overbrace{(I \otimes \langle l|)U_B^{QE_B}(|e_B\rangle \otimes I)}^{B_l} \otimes \langle j|n_B\rangle\bigg)(\rho^C \otimes \rho^Q) \\
&\times \bigg(|0\rangle\langle 0|^C \otimes \langle n_A|k\rangle \otimes \overbrace{(\langle e_A| \otimes I)U_A^{E_A Q\dagger}(|i\rangle \otimes I)}^{A_i^\dagger}\,\overbrace{(I \otimes \langle n_B|)U_B^{QN_B\dagger}(I \otimes |j\rangle)}^{B_j^\dagger} \otimes \langle e_B|l\rangle
\end{aligned}
$$

$$+ |1\rangle\langle 1|^C \otimes \langle e_A|i\rangle \otimes \overbrace{(\langle n_A| \otimes I)U_A^{N_AQ\dagger}(|k\rangle \otimes I)}^{A_k^\dagger}\overbrace{(I \otimes \langle e_B|)U_B^{QE_B\dagger}(|l\rangle \otimes I)}^{B_l^\dagger} \otimes \langle n_B|j\rangle\Big)$$

$$= \sum_{i,j,k,l}^{d^2} \frac{1}{d^4}(|0\rangle\langle 0|^C \otimes B_jA_i + |1\rangle\langle 1|^C \otimes A_kB_l)(\rho^C \otimes \rho^Q)(|0\rangle\langle 0|^C \otimes A_i^\dagger B_j^\dagger + |1\rangle\langle 1|^C \otimes B_l^\dagger A_k^\dagger)$$

$$= \sum_{i,j,k,l}^{d^2} K_{ijkl}^{\text{traj}}(\rho^C \otimes \rho^Q)K_{ijkl}^{\text{traj}\dagger}. \tag{A2}$$

[1] C. H. Bennett and S. J. Wiesner, Communication via One- and Two-Particle Operators on Einstein-Podolsky-Rosen States, Phys. Rev. Lett. **69**, 2881 (1992).

[2] C. H. Bennett, G. Brassard, C. Crépeau, R. Jozsa, A. Peres, and W. K. Wootters, Teleporting an Unknown Quantum State Via Dual Classical and Einstein-Podolsky-Rosen Channels, Phys. Rev. Lett. **70**, 1895 (1993).

[3] B. Schumacher, Sending entanglement through noisy quantum channels, Phys. Rev. A **54**, 2614 (1996).

[4] P. Hausladen, R. Jozsa, B. Schumacher, M. Westmoreland, and W. K. Wootters, Classical information capacity of a quantum channel, Phys. Rev. A **54**, 1869 (1996).

[5] B. Schumacher and M. A. Nielsen, Quantum data processing and error correction, Phys. Rev. A **54**, 2629 (1996).

[6] B. Schumacher and M. D. Westmoreland, Sending classical information via noisy quantum channels, Phys. Rev. A **56**, 131 (1997).

[7] A. Holevo, The capacity of the quantum channel with general signal states, IEEE Trans. Inf. Theory **44**, 269 (1998).

[8] S. Lloyd, Capacity of the noisy quantum channel, Phys. Rev. A **55**, 1613 (1997).

[9] I. Devetak, The private classical capacity and quantum capacity of a quantum channel, IEEE Trans. Inf. Theory **51**, 44 (2005).

[10] D. P. DiVincenzo, P. W. Shor, and J. A. Smolin, Quantum-channel capacity of very noisy channels, Phys. Rev. A **57**, 830 (1998).

[11] M. B. Hastings, Superadditivity of communication capacity using entangled inputs, Nat. Phys. **5**, 255 (2009).

[12] G. Smith and J. Yard, Quantum communication with zero-capacity channels, Science **321**, 1812 (2008).

[13] O. Oreshkov, F. Costa, and Č. Brukner, Quantum correlations with no causal order, Nat. Commun. **3**, 1092 (2012).

[14] G. Chiribella, G. M. D'Ariano, P. Perinotti, and B. Valiron, Quantum computations without definite causal structure, Phys. Rev. A **88**, 022318 (2013).

[15] G. Chiribella, Perfect discrimination of no-signalling channels via quantum superposition of causal structures, Phys. Rev. A **86**, 040301(R) (2012).

[16] M. Araújo, F. Costa, and Č. Brukner, Computational Advantage from Quantum-Controlled Ordering of Gates, Phys. Rev. Lett. **113**, 250402 (2014).

[17] M. J. Renner and Č. Brukner, Computational Advantage from a Quantum Superposition of Qubit Gate Orders, Phys. Rev. Lett. **128**, 230503 (2022).

[18] C. Mukhopadhyay, M. K. Gupta, and A. K. Pati, Superposition of causal order as a metrological resource for quantum thermometry, arXiv:1812.07508.

[19] X. Zhao and C. Giulio, Advantage of indefinite causal order in quantum metrology, in *Quantum Information and Measurement (QIM) V: Quantum Technologies* (OSA, Rome, 2019), p. F5A.23.

[20] X. Zhao, Y. Yang, and G. Chiribella, Quantum Metrology with Indefinite Causal Order, Phys. Rev. Lett. **124**, 190503 (2020).

[21] D. Felce and V. Vedral, Quantum Refrigeration with Indefinite Causal Order, Phys. Rev. Lett. **125**, 070603 (2020).

[22] K. Simonov, G. Francica, G. Guarnieri, and M. Paternostro, Work extraction from coherently activated maps via quantum switch, Phys. Rev. A **105**, 032217 (2022).

[23] A. Feix, M. Araújo, and Č. Brukner, Quantum superposition of the order of parties as a communication resource, Phys. Rev. A **92**, 052326 (2015).

[24] P. A. Guérin, A. Feix, M. Araújo, and Č. Brukner, Exponential Communication Complexity Advantage from Quantum Superposition of the Direction of Communication, Phys. Rev. Lett. **117**, 100502 (2016).

[25] N. Loizeau and A. Grinbaum, Channel capacity enhancement with indefinite causal order, Phys. Rev. A **101**, 012340 (2020).

[26] A. Mitra, H. Badhani, and S. Ghosh, Improvement in quantum communication using quantum switch, arXiv:2108.14001.

[27] D. Ebler, S. Salek, and G. Chiribella, Enhanced Communication with the Assistance of Indefinite Causal Order, Phys. Rev. Lett. **120**, 120502 (2018).

[28] G. Chiribella, M. Banik, S. S. Bhattacharya, T. Guha, M. Alimuddin, A. Roy, S. Saha, S. Agrawal, and G. Kar, Indefinite causal order enables perfect quantum communication with zero capacity channels, New J. Phys. **23**, 033039 (2021).

[29] L. M. Procopio, F. Delgado, M. Enríquez, N. Belabas, and J. A. Levenson, Communication enhancement through quantum coherent control of *N* channels in an indefinite causal-order scenario, Entropy **21**, 1012 (2019).

[30] S. Sazim, M. Sedlak, K. Singh, and A. K. Pati, Classical communication with indefinite causal order for depolarizing channels, Phys. Rev. A **103**, 062610 (2021).

[31] A. A. Abbott, J. Wechs, D. Horsman, M. Mhalla, and C. Branciard, Communication through coherent control of quantum channels, Quantum **4**, 333 (2020).

[32] P. A. Guérin, G. Rubino, and Č. Brukner, Communication through quantum-controlled noise, Phys. Rev. A **99**, 062317 (2019).

[33] G. Chiribella and H. Kristjánsson, Quantum Shannon theory with superpositions of trajectories, Proc. R. Soc. A **475**, 20180903 (2019).

[34] H. Kristjánsson, G. Chiribella, S. Salek, D. Ebler, and M. Wilson, Resource theories of communication, New J. Phys. **22**, 073014 (2020).

[35] L. M. Procopio, A. Moqanaki, M. Araújo, F. Costa, I. Alonso Calafell, E. G. Dowd, D. R. Hamel, L. A. Rozema, Č. Brukner, and P. Walther, Experimental superposition of orders of quantum gates, Nat. Commun. **6**, 7913 (2015).

[36] G. Rubino, L. A. Rozema, A. Feix, M. Araújo, J. M. Zeuner, L. M. Procopio, Č. Brukner, and P. Walther, Experimental verification of an indefinite causal order, Sci. Adv. **3**, e1602589 (2017).

[37] K. Goswami, C. Giarmatzi, M. Kewming, F. Costa, C. Branciard, J. Romero, and A. G. White, Indefinite Causal Order in a Quantum Switch, Phys. Rev. Lett. **121**, 090503 (2018).

[38] G. Rubino, L. A. Rozema, D. Ebler, H. Kristjánsson, S. Salek, P. Allard Guérin, Č. Brukner, A. A. Abbott, C. Branciard, G. Chiribella, and P. Walther, Experimental quantum communication enhancement by superposing trajectories, Phys. Rev. Res. **3**, 013093 (2021).

[39] N. Paunković and M. Vojinović, Causal orders, quantum circuits and spacetime: Distinguishing between definite and superposed causal orders, Quantum **4**, 275 (2020).

[40] Á. Rivas, S. F. Huelga, and M. B. Plenio, Quantum non-Markovianity: Characterization, quantification and detection, Rep. Prog. Phys. **77**, 094001 (2014).

[41] C. Pineda, T. Gorin, D. Davalos, D. A. Wisniacki, and I. García-Mata, Measuring and using non-Markovianity, Phys. Rev. A **93**, 022117 (2016).

[42] H. Kristjánsson, W. Mao, and G. Chiribella, Witnessing latent time correlations with a single quantum particle, Phys. Rev. Res. **3**, 043147 (2021).

[43] S. Milz, F. A. Pollock, T. P. Le, G. Chiribella, and K. Modi, Entanglement, non-Markovianity, and causal non-separability, New J. Phys. **20**, 033033 (2018).

[44] P. Chawla, U. Shrikant, and C. M. Chandrashekar, Superposition of causal order in quantum walks: Non-Markovianity and causal asymmetry, arXiv:2205.13217.

[45] J. Naikoo, S. Banerjee, and C. M. Chandrashekar, Non-Markovian channel from the reduced dynamics of a coin in a quantum walk, Phys. Rev. A **102**, 062209 (2020).

[46] M. J. W. Hall, J. D. Cresser, L. Li, and E. Andersson, Canonical form of master equations and characterization of non-Markovianity, Phys. Rev. A **89**, 042120 (2014).

[47] A. G. Maity and S. Bhattacharya, Activating hidden non-Markovianity with the assistance of quantum SWITCH, arXiv:2206.04524.

[48] D. Petz, Quasi-entropies for finite quantum systems, Rep. Math. Phys. **23**, 57 (1986).

[49] G. Lindblad, On the generators of quantum dynamical semigroups, Commun. Math. Phys. **48**, 119 (1976).

[50] V. Gorini, Completely positive dynamical semigroups of N-level systems, J. Math. Phys. **17**, 821 (1976).

[51] Á. Rivas, S. F. Huelga, and M. B. Plenio, Entanglement and Non-Markovianity of Quantum Evolutions, Phys. Rev. Lett. **105**, 050403 (2010).

[52] H.-P. Breuer, E.-M. Laine, and J. Piilo, Measure for the Degree of Non-Markovian Behavior of Quantum Processes in Open Systems, Phys. Rev. Lett. **103**, 210401 (2009).

[53] S. Wißmann, H.-P. Breuer, and B. Vacchini, Generalized trace-distance measure connecting quantum and classical non-Markovianity, Phys. Rev. A **92**, 042108 (2015).

[54] H.-P. Breuer, E.-M. Laine, J. Piilo, and B. Vacchini, *Colloquium*: Non-Markovian dynamics in open quantum systems, Rev. Mod. Phys. **88**, 021002 (2016).

[55] G. Lindblad, Completely positive maps and entropy inequalities, Commun. Math. Phys. **40**, 147 (1975).

[56] M. B. Ruskai, Beyond strong subadditivity? improved bounds on the contraction of generalized relative entropy, Rev. Math. Phys. **06**, 1147 (1994).

[57] X.-M. Lu, X. Wang, and C. P. Sun, Quantum Fisher information flow and non-Markovian processes of open systems, Phys. Rev. A **82**, 042103 (2010).

[58] P. Abiuso, M. Scandi, J. Surace, and D. D. Santis, Characterizing non-Markovianity through fisher information, arXiv:2204.04072.

[59] D. Chruściński, A. Kossakowski, and Á. Rivas, Measures of non-Markovianity: Divisibility versus backflow of information, Phys. Rev. A **83**, 052128 (2011).

[60] P. Pechukas, Reduced Dynamics Need not be Completely Positive, Phys. Rev. Lett. **73**, 1060 (1994).

[61] R. Alicki, Comment on "Reduced Dynamics Need not be Completely Positive", Phys. Rev. Lett. **75**, 3020 (1995).

[62] L.-p. Han, J. Zou, H. Li, and B. Shao, Quantum information scrambling in non-markovian open quantum systems, arXiv:2205.03979.

[63] N. Dowling, P. Figueroa-Romero, F. A. Pollock, P. Strasberg, and K. Modi, Equilibration of non-markovian quantum processes in finite time intervals, arXiv:2112.01099.

[64] F. F. Fanchini, G. Karpat, B. Çakmak, L. K. Castelano, G. H. Aguilar, O. J. Farías, S. P. Walborn, P. H. Souto Ribeiro, and M. C. de Oliveira, Non-Markovianity through Accessible Information, Phys. Rev. Lett. **112**, 210402 (2014).

[65] C. Bennett, A. Harrow, D. Leung, and J. Smolin, On the capacities of bipartite Hamiltonians and unitary gates, IEEE Trans. Inf. Theory **49**, 1895 (2003).

[66] D. W. Berry and B. C. Sanders, Relation between classical communication capacity and entanglement capability for two-qubit unitary operations, Phys. Rev. A **68**, 032312 (2003).

[67] V. Coffman, J. Kundu, and W. K. Wootters, Distributed entanglement, Phys. Rev. A **61**, 052306 (2000).

[68] G. Gour and Y. Guo, Monogamy of entanglement without inequalities, Quantum **2**, 81 (2018).

[69] T. J. Osborne and F. Verstraete, General Monogamy Inequality for Bipartite Qubit Entanglement, Phys. Rev. Lett. **96**, 220503 (2006).

[70] B. Kraus and J. I. Cirac, Optimal creation of entanglement using a two-qubit gate, Phys. Rev. A **63**, 062309 (2001).

[71] P. Zanardi, Entanglement of quantum evolutions, Phys. Rev. A **63**, 040304(R) (2001).

[72] X. Wang and P. Zanardi, Quantum entanglement of unitary operators on bipartite systems, Phys. Rev. A **66**, 044303 (2002).

[73] M. A. Nielsen, C. M. Dawson, J. L. Dodd, A. Gilchrist, D. Mortimer, T. J. Osborne, M. J. Bremner, A. W. Harrow, and A. Hines, Quantum dynamics as a physical resource, Phys. Rev. A **67**, 052301 (2003).

[74] L. Chen and L. Yu, Entangling and assisted entangling power of bipartite unitary operations, Phys. Rev. A **94**, 022307 (2016).

[75] D. Felce, N. T. Vidal, V. Vedral, and E. O. Dias, Indefinite causal orders from superpositions in time, Phys. Rev. A **105**, 062216 (2022).

[76] G. Tóth, T. Moroder, and O. Gühne, Evaluating Convex Roof Entanglement Measures, Phys. Rev. Lett. **114**, 160501 (2015).

[77] S. Khatri and M. M. Wilde, Principles of quantum communication theory: A modern approach, arXiv:2011.04672.

[78] M. Horodecki, P. W. Shor, and M. B. Ruskai, Entanglement breaking channels, Rev. Math. Phys. **15**, 629 (2003).

[79] M. Zych, F. Costa, I. Pikovski, T. C. Ralph, and Č. Brukner, General relativistic effects in quantum inter-

ference of photons, Class. Quantum Grav. **29**, 224010 (2012).

[80] A. Feix and Č. Brukner, Quantum superpositions of 'common-cause' and 'direct-cause' causal structures, New J. Phys. **19**, 123028 (2017).

[81] A. Belenchia, R. M. Wald, F. Giacomini, E. Castro-Ruiz, Č. Brukner, and M. Aspelmeyer, Quantum superposition of massive objects and the quantization of gravity, Phys. Rev. D **98**, 126009 (2018).

[82] M. Zych, F. Costa, I. Pikovski, and Č. Brukner, Bell's theorem for temporal order, Nat. Commun. **10**, 3772 (2019).